

AD-A953 719

DTIC ACCESSION NUMBER

LEVEL

PHOTOGRAPH THIS SHEET

INVENTORY

WAL - 244

DOCUMENT IDENTIFICATION

14 Jan. 37

DISTRIBUTION STATEMENT A

Approved for public release;
Distribution Unlimited

DISTRIBUTION STATEMENT

ACCESSION FOR	
NTIS	GRA&I
DTIC	TAB
UNANNOUNCED	
JUSTIFICATION	
BY	
DISTRIBUTION	
AVAILABILITY CODES	
DIST	AVAIL AND/OR SPECIAL
71	244

DISTRIBUTION STAMP

UNANNOUNCED

84 10 12 047

DATE RECEIVED IN DTIC

DTIC	
ELECTE	
S	NOV 7 1984
D	

DATE ACCESSIONED

DATE RETURNED

REGISTERED OR CERTIFIED NO.

PHOTOGRAPH THIS SHEET AND RETURN TO DTIC-DDAC

**Best
Available
Copy**

UNCLASSIFIED

POST. Lab.
WATERTOWN ARSENAL
WATERTOWN, MASS.

LABORATORY

INDEXED



REPORT NO. 710/197

CONFIDENTIAL

DAM

AD-A953 719

A STUDY OF
THE MECHANISM OF PENETRATION OF HOMOGENEOUS
ARMOR PLATE

INDEXED

By

E. L. REED
Research Metallurgist

S. L. KRUEGEL
Jr. Phys. Sci. Aide

UNCLASSIFIED

June 14, 1937

WATERTOWN ARSENAL
WATERTOWN, MASS.

UNCLASSIFIED

DISTRIBUTION OF REPORTS

REPORT NO. 710/177 TITLE _____DATE DISTRIBUTED 6/30/37 _____

	Lo- cal	Other Ord. Work	Army	Navy	Private
Author	1 ✓	1	1	1	1
Lab File	1 ✓	1	1	1	1
Main Office File	1 ✓	1	1	1	1
Chief of Ordnance	2 ✓	2	2	2	2
Technical Staff	1	1	1	1	1
Springfield Armory	1	1	1	1	1
Watervliet Arsenal	1	1	1	1	1
Rock Island Arsenal	1	1	1	1	1
Frankford Arsenal	1	1	1	1	1
Picatinny Arsenal	1	1	1	1	1
Aberdeen Proving Ground	1	1	1	1	1
Chief, Bureau Ordnance	1	1	1	1	1
Naval Gun Factory	1	1	1	1	1
Chief, Bureau C & R	1	1	1	1	1
Local Circulation	1	1	1	1	1
Available for special circulation.	2	2	3	3	1
Other establishments requesting work.	2	2	2	2	2
Private Parties paying for work	2	2	2	2	2

UNCLASSIFIED

UNCLASSIFIED

THIS REPORT AVAILABLE IN MICROFICHE ONLY

UNCLASSIFIED

Report No. 710/197
Watertown Arsenal

June 14, 1937

~~CONFIDENTIAL~~

A STUDY OF
THE MECHANISM OF PENETRATION OF HOMOGENEOUS
ARMOR PLATE

Purpose

The purpose of this investigation was to study the nature of deformation in partially and completely penetrated homogeneous armor plate when subjected to impact with armor piercing ammunition.

Conclusions

1. Armor piercing bullets penetrate homogeneous armor plate by means of a punching and boring operation. The compressed metal under bullet impact is in many cases partially forced back to the surface, forming the well known craters.
2. The boring action of the bullet has caused a torsional flow pattern in the armor plate in the vicinity of the bullet hole. The torsional flow of the metal is in the same direction as the rotation of the bullet. The contour of the area disturbed and twisted by the bullet is of the hour-glass shape, the necking-in being at the ogive. In several cases spiral markings were found on the bullet cores.

UNCLASSIFIED

3. When an armor piercing bullet penetrates armor plate, the following facts are to be considered:

- (a) Some of the energy of the bullet is dissipated into heat, causing a local rise in temperature in the plate.
- (b) Local deformation or faulting of the metal progresses along planes of greatest slip stress, which would normally be at 45 degrees, to the direction of impact; but in this case, due to the rotational effects of the bullet, they are of random orientation.
- (c) Sufficient heat has been generated to raise the temperature of these localized slip areas above the critical, or in some cases, even to the melting point. The sudden chilling of these areas form layers which are referred to as "white layers".
- (d) These "white layers" identify themselves as martensite in their physical properties, but do not possess the typical martensitic structure.

4. The occurrence of "white layers" in armor plate:

- (a) They are present in the area immediately surrounding the bullet hole in both high and low ballistic plate of various compositions.

(b) The more nearly the steel approaches a true martensitic condition, the greater the concentration of the "white layer" becomes, i.e. the harder the plate, the more concentrated the layers.

5. In general, the greater the ballistic resistance, the more "white layers" occur.

6. The impact of ball ammunition on armor plate is a straight punching operation. No boring action is evident. "White layer" occurs at surface of slip between the punching and the body of the plate.

7. Patterns, which resemble strain markings in characteristic Lüder formation, were revealed on the back faces of some armor plates by flaking off of scale while plate was being subjected to bullet impact.

8. High power microscopic examination of the "white layer" present in the standard composition made under oblique illumination shows flow lines within and immediately adjacent to the layer. The surface of the layer was not a flat smoothly finished face but rather irregularly furrowed.

9. Crack systems within and closely associated with "white layers" are of the following types:

- (a) Hair-line cracks within the "white layer".
- (b) Pronounced cracks partially within the "white layer", either propagated by a tearing or

twisting of the metal. (This latter type comprises about one-third of all the cracks found in the layers).

- (c) Rare, isolated cracks crossing "white layers".
- (d) Crack systems with no special relationship to "white layers".

10. (a) High Power microscopic examination reveals, in some cases, the presence of clear cut nonmetallic inclusions which were intact within the "white layers". However, the absence, in general, of nonmetallics within the "white layer" may indicate a possibility of sufficient heat having been generated in these slip planes to melt the inclusions which normally would occur in these areas.

- (b) On the other hand, many nonmetallics of the elongated type adjacent to or partially within the "white layer" were distorted but not fused.

11. Dark layers, similar in orientation to the "white layers" of standard plate, were found in Hadfield's Austenitic Manganese steel (a poor ballistic plate). However, these layers consisted of carbide precipitates and alpha iron, showing that due to intense heat generated within these slip areas, a phase change had taken place.

12. No "white layer" was developed by bullet penetrations in rolled low carbon steel plate.

13. Carbide precipitation in the outer surface of the bullet core is caused by the heat developed during bullet impact.

14. In the samples examined, no evidence of fusion of the metal at the edge of the bullet hole was detected in homogeneous armor plate. Likewise, no fusion was evident in the bullet core.

15. Hardness surveys in the vicinity of bullet holes indicated:

- (a) That about .25 inch of metal around the bullet hole is work hardened.
- (b) In complete penetrations, maximum hardness is found at the entrance side of the plate.
- (c) In partial penetrations, maximum hardness is found at the contour of the bullet hole representing the ogive and extending around the tip of the hole.
- (d) In the case of partially penetrated armor plate containing 3.5% Nickel and 2.4% Silicon, maximum hardness was found .005 inch below the tip of the bullet hole.

- (e) In some cases, metal deformed near bullet impact as revealed by macro-etching, was decidedly work hardened.

Experimental Procedure

Several homogeneous plates and one cast plate were selected for examination as follows:

- (a) Plate No. 29 - High ballistic properties.
Size 12 x 12 x 1 inch - Manufacturer-Henry Disston & Sons, Inc.
- (b) Plate No. WJ2 - High ballistic properties.
Size 12 x 12 x 1/2 inch - Manufacturer-Jessop Steel Co.
- (c) Plate No. Ex 26 - Medium ballistic properties.
Size 12 x 12 x 1/2"- Manufacturer-Henry Disston & Sons, Inc.
- (d) Plate No. 614-6 - Medium ballistic properties.
Size 12 x 12 x 1/2 inch - Manufacturer-Watertown Arsenal-Henry Disston & Sons Co., Inc., Order 8542, Ingot 12-614.
- (e) Plate No. 2 - Poor ballistic properties.
Size 12 x 12 x 1/2 - Manufacturer-Taylor-Wharton Co.
- (f) Cast Carburetor Cover No. A - Poor ballistic properties.
Size 21 1/2 x 15 x 1/2 inch - Manufacturer-Watertown Arsenal.

Representative partial and complete penetrations in each of the above plates were sectioned. A study of the macro-structure and microstructure at the area of bullet impact was made.

Chemical analysis was made on several plates, the analyses of which were not recorded in the reports submitted by Aberdeen Proving Ground.

Spectrographic analysis was made on samples cut from all plates, except No. 2 and No. A.

The ballistic properties of the plates, as determined at Aberdeen Proving Ground, are found in the following Partial Reports on Test of Thin Armor Plate: 21, 59, 81, 82 and 96.

Experimental Results

1. Spectrographic Analysis

Spectrographic analyses of the plates examined are given in Table 1.

Table 1
Spectrographic Analysis

Element	Plate No:			
	29	WJ2	Ex 26	614-5
Ni	Present	Faint Trace	Trace	Trace
Cu	Trace	Present	Present	Present
Al	Trace	Trace	Trace	Faint Trace
Ti	Trace	Trace	Trace	Trace
Ca	Faint Trace	Faint Trace	Faint Trace	Faint Trace
Sn	Trace	Trace	Trace	Trace

2. Heat Treatment of Plates

The heat treatment given the plates by the manufacturers is stated in Table 2.

Table 2
Heat Treatment of Plates

<u>Plate No.</u>	<u>Heated to</u>	<u>Quenching Medium</u>	<u>Draw</u>
29	1575°F	Not stated	1075°F
WJ2	Not stated	Not stated	Not stated
Ex 26	1700°F	Oil	1150°F
614-5	1650°F	Oil	1150°F
2	Not stated	Not stated	Not stated
Cast "A"	Heated 8 hours to 2102°F, air cooled.		
	Heated 5 hours at 1742°F, air cooled.		
	Heated 5 hours at 1562°F, furnace cooled.		
	Heated 2 hours at 1600°F, oil quenched.		
	Drawn 2 hours at 925°F, air cooled.		

3. Chemical Analysis

The chemical analyses of the several plates examined are given in Table 3.

Table 3
Chemical Analysis

<u>Plate No.</u>	<u>C</u>	<u>Mn</u>	<u>P</u>	<u>S</u>	<u>Si</u>	<u>Ni</u>	<u>Cr</u>	<u>Mo</u>	<u>Va</u>	<u>Cu</u>
29	.50	.70	.025	.020	.25	-	1.12	.65	.25	.312
WJ2	.425	.66	.024	.018	2.01	3.58	.24	-	-	-
Ex 26	.38	.69	-	.17	-	-	1.14	.65	.30	.296
614-5	.51	.42	.016	.013	.14	.09	1.21	.56	.29	.252
2	1.17	11.40	.057	.018	.405	-	-	-	-	-
Cast "A"	.19	.54	.010	.018	.165	-	1.13	.82	.21	-

4. Ballistic Properties

The ballistic properties of the plates as determined at Aberdeen Proving Ground are given in Table 4.

5. Macroscopic and Microscopic Examinations

Typical macro- and microstructures of deformation at penetrations in armor plate are shown in Figures 1 - 21, inclusive.

6. Hardness Surveys

Vickers-Brinell hardness surveys were made in the vicinity of typical penetrations and the results plotted, as shown in Figures 23 - 51.

Table 4

Ballistic Properties

Plate No.	Thickness	Brinell Hardness	Ballistic Limit			Manufacturer
			Spec. 31 f.s.	ft.lbs.	AXS-54 f.s.	
29	1"	418	-	-	*2568	10985 Henry Disston & Sons, Inc. Cal .50 M-1 - 100 yards.
WJ2	1/2"	555	**2945	-	-	- Jessop Manufacturing Co. Cal .30 A.P. M-1922- 100 yards.
Ex 26	1/2"	402-418	2700	2671	2380	2075 Henry Disston & Sons, Inc. Cal .30 A.P. M-1922-100 yds
614-5	1/2"	430-444	2685	2642	2451	2201 Watertown Arsenal-Henry Disston & Sons, Inc. Cal .30 A.P. M-1922, 100 yds
2	1/2"	255	2252	1858	-	- Taylor Wharton Co. Cal.30 A.P. M-1922-50 yds.
Cast "A"	1/2"	418	-	-	1897	1312 Watertown Arsenal - Cal.30 A.P. M-1922 - 100 yards.

*Withstood Cal .50 A.P. M-1 Ammunition at distance of 100 yards.

**Withstood Cal .30 A.P. M-1922 Ammunition at distance of 100 yards.

Discussion

Macrostructure

When armor plate of the homogeneous type is either partially or completely penetrated by armor piercing bullets, several types of deformation or flow lines are detected in the area of impact. Figures 1, 2, and 3 illustrate the macrostructures of sections cut through bullet holes after etching in a standard macroetching reagent.

In the first place, the banded structure is deformed in the vicinity of the bullet hole. Banded structures in plate are the result of deforming the dendritic segregation present in the ingot, this segregation being elongated in the direction of hot-work.

Furthermore, a second type of flow line or "white layer" is observed which resists etching according to the normal macroetching practice, and is not oriented in any particular direction with respect to the axis of the bullet hole.

This "white layer" was detected in standard rolled and cast chromium-molybdenum-vanadium plates of high and medium ballistic properties, and also in a high ballistic plate containing 3.58% nickel and 2.01% silicon.

Cast plate of the standard chromium-molybdenum-vanadium composition and of low ballistic properties showed this type of deformation at the penetrated area.

Figure 1

Plate No. 29

Macrostructure of partial penetration
of .50 Caliber A.P. bullet into high ballis-
tic plate shows deformation of banding and
"white layer".

Etch: Rosenhain & Haughton #29, Round 3

MA 378_a, c

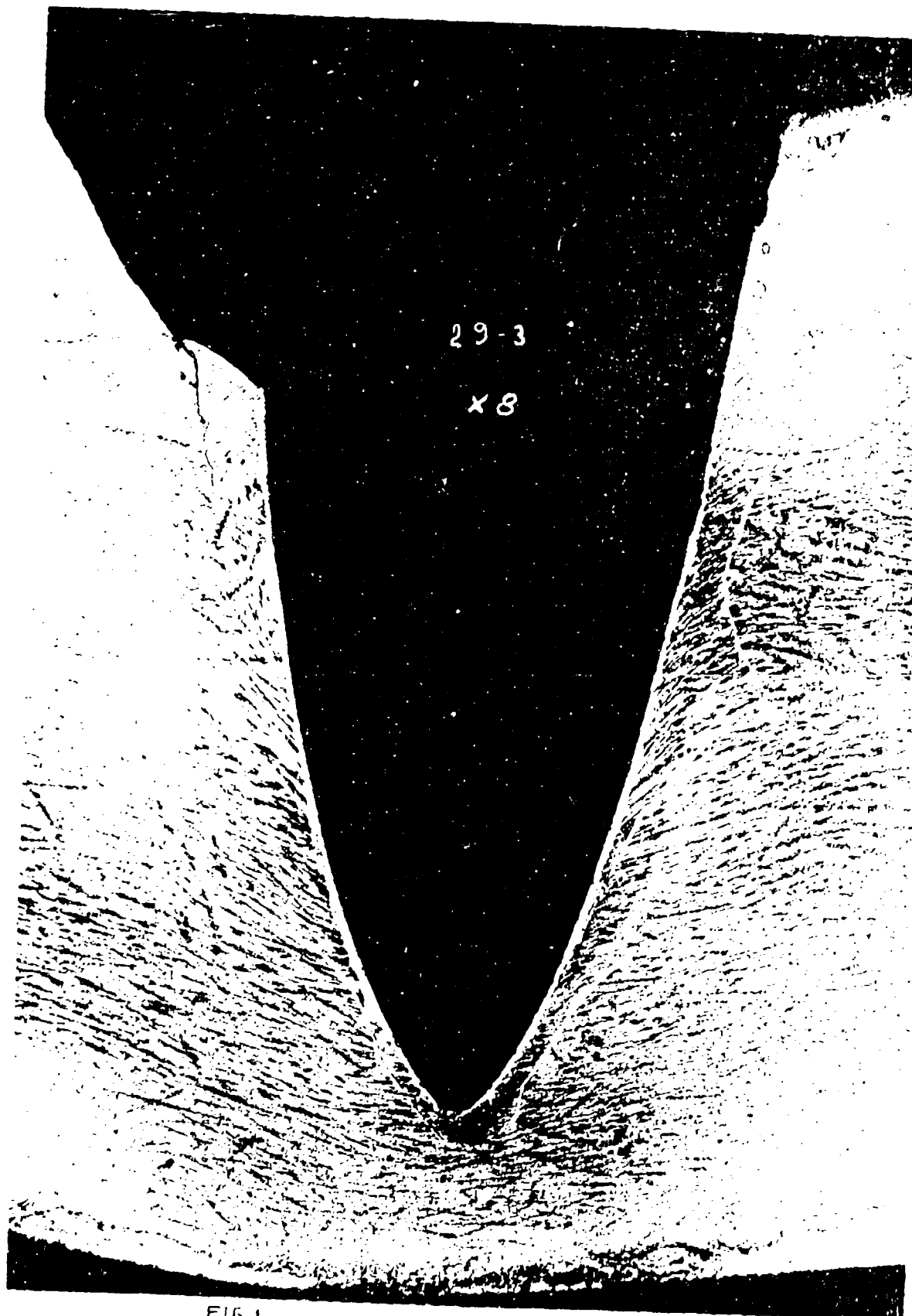


FIG 1

WALSH 611

Figure 2

Plate Ex 26

(a) Spalling and deformation of banding, as well as "white layer" formation, are indicated in this macrostructure of a complete penetration of .30 caliber A.P. bullet into medium ballistic plate.

#Ex 26 Round 4 - MA 383_{a, b}

(b) Shows partial penetration of same plate.

#Ex 26 Round 7 - MA 381

Both etched in Rosenhain & Haughton's reagent.

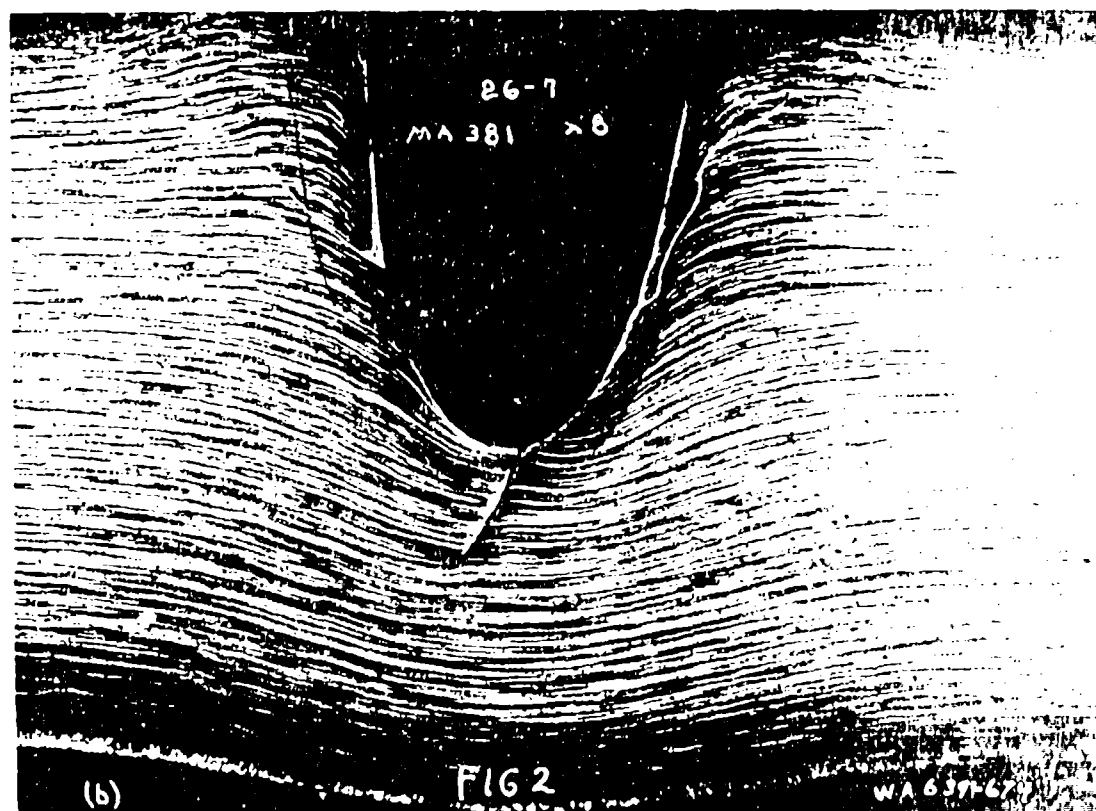
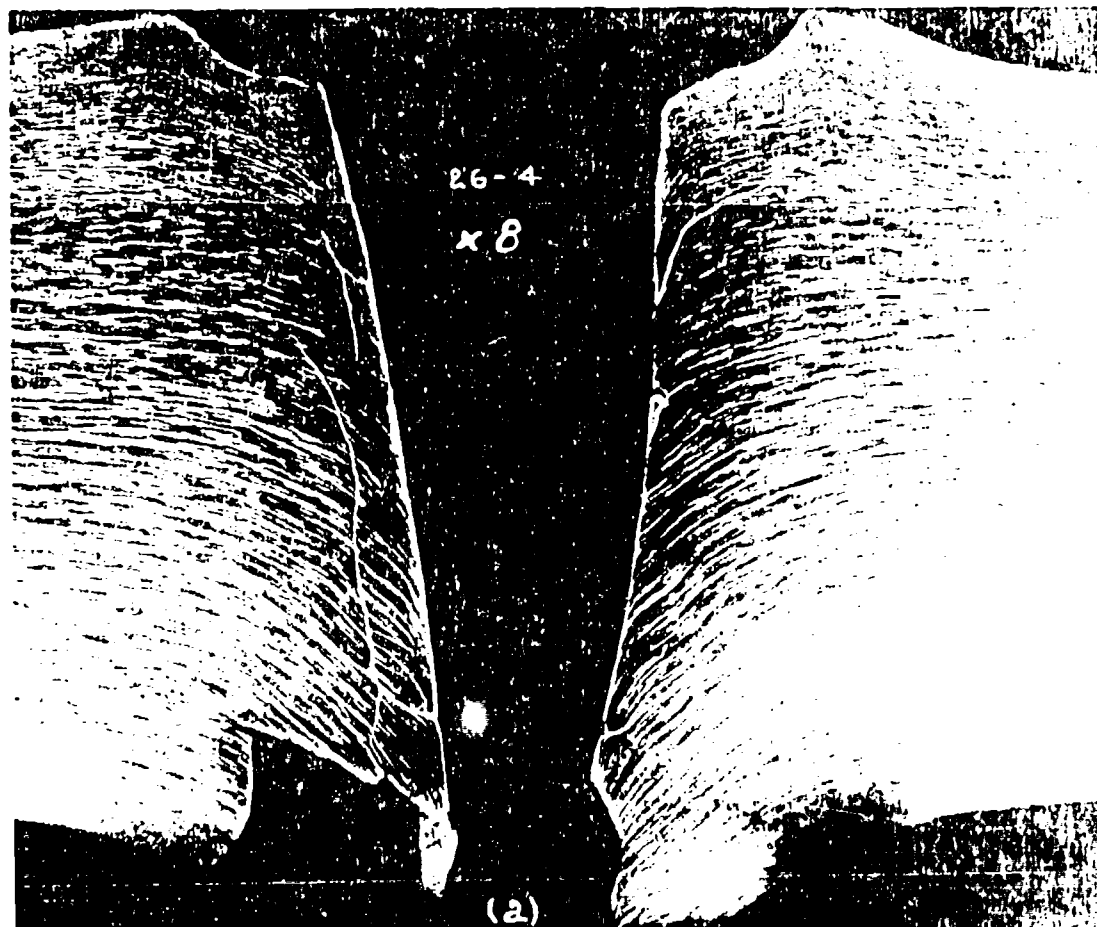


Figure 3

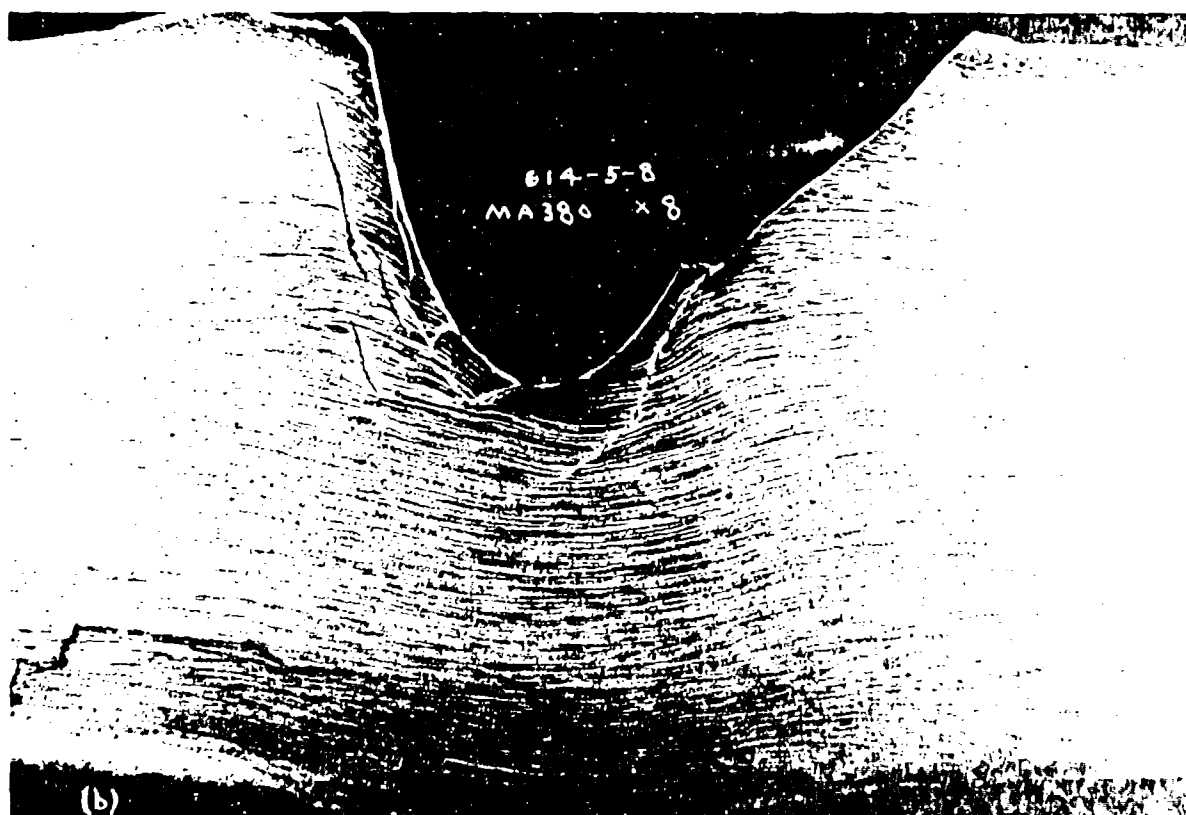
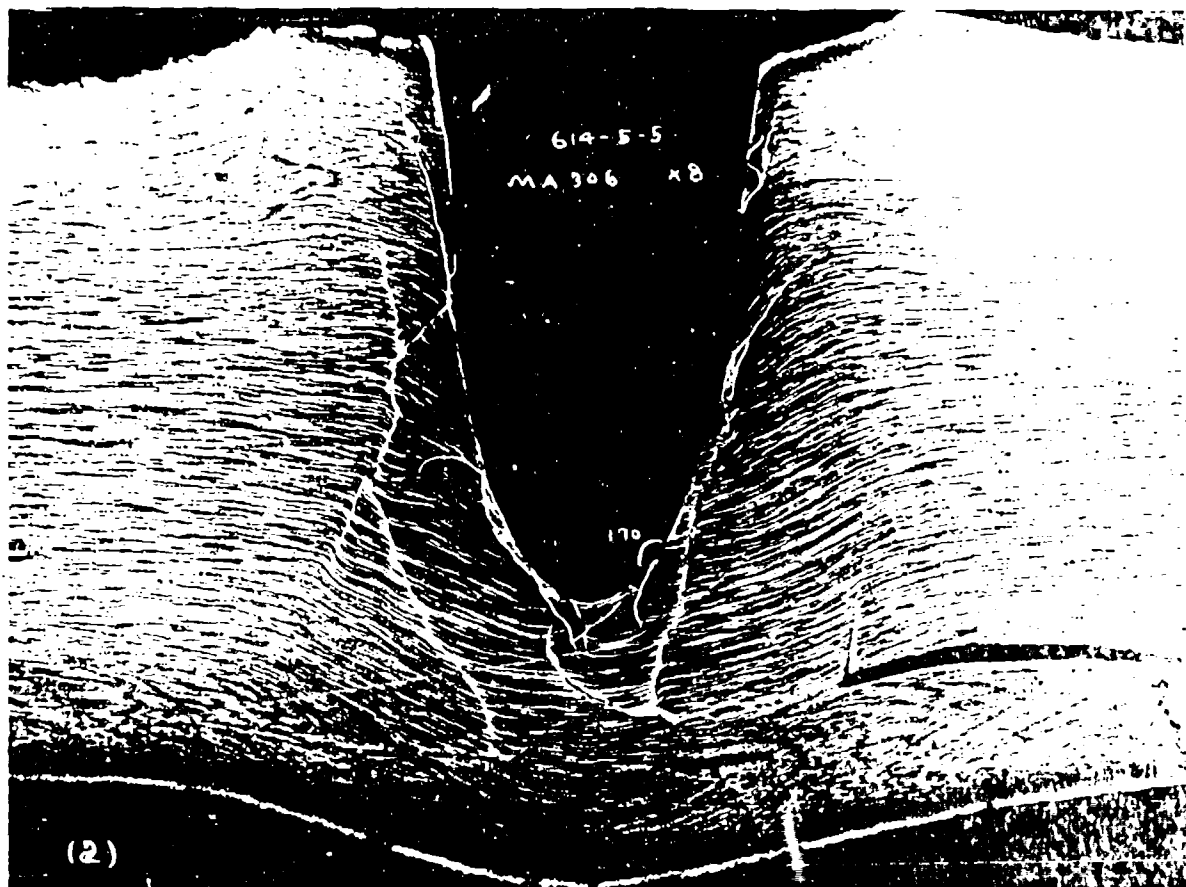
Plate No. 614-5

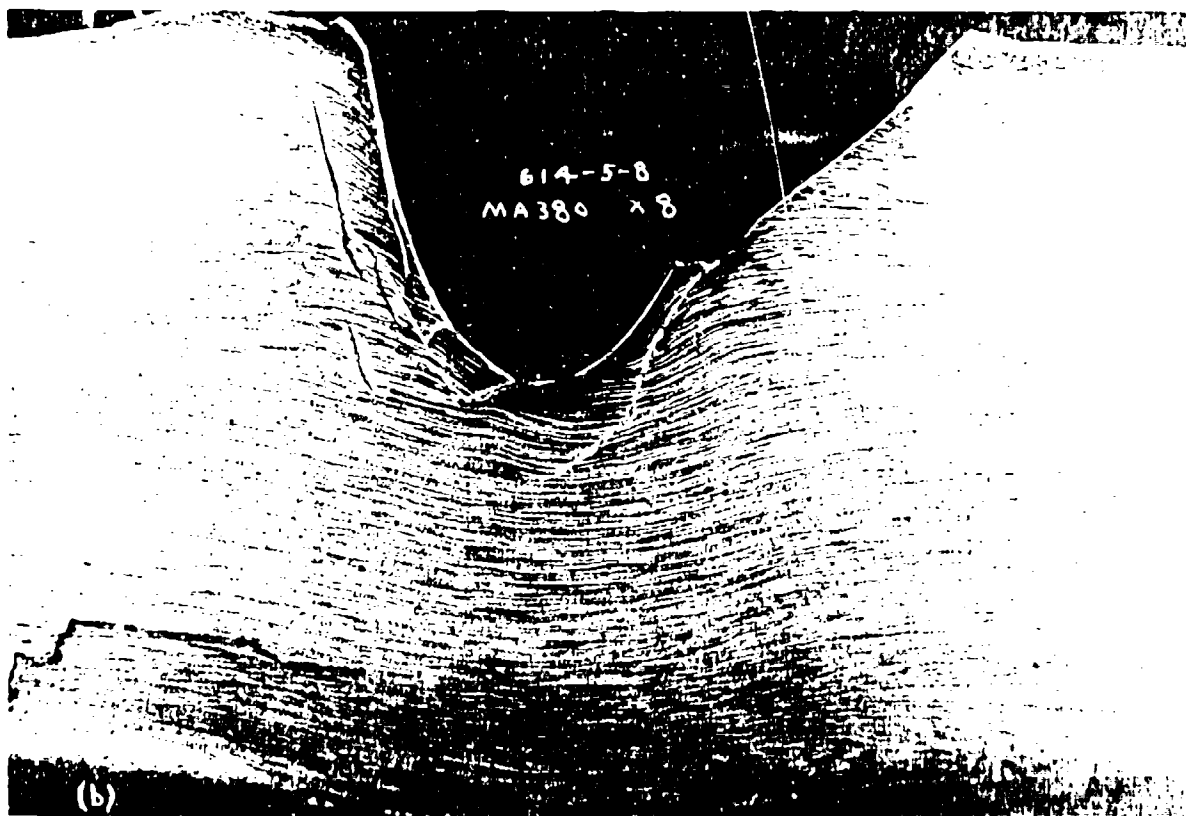
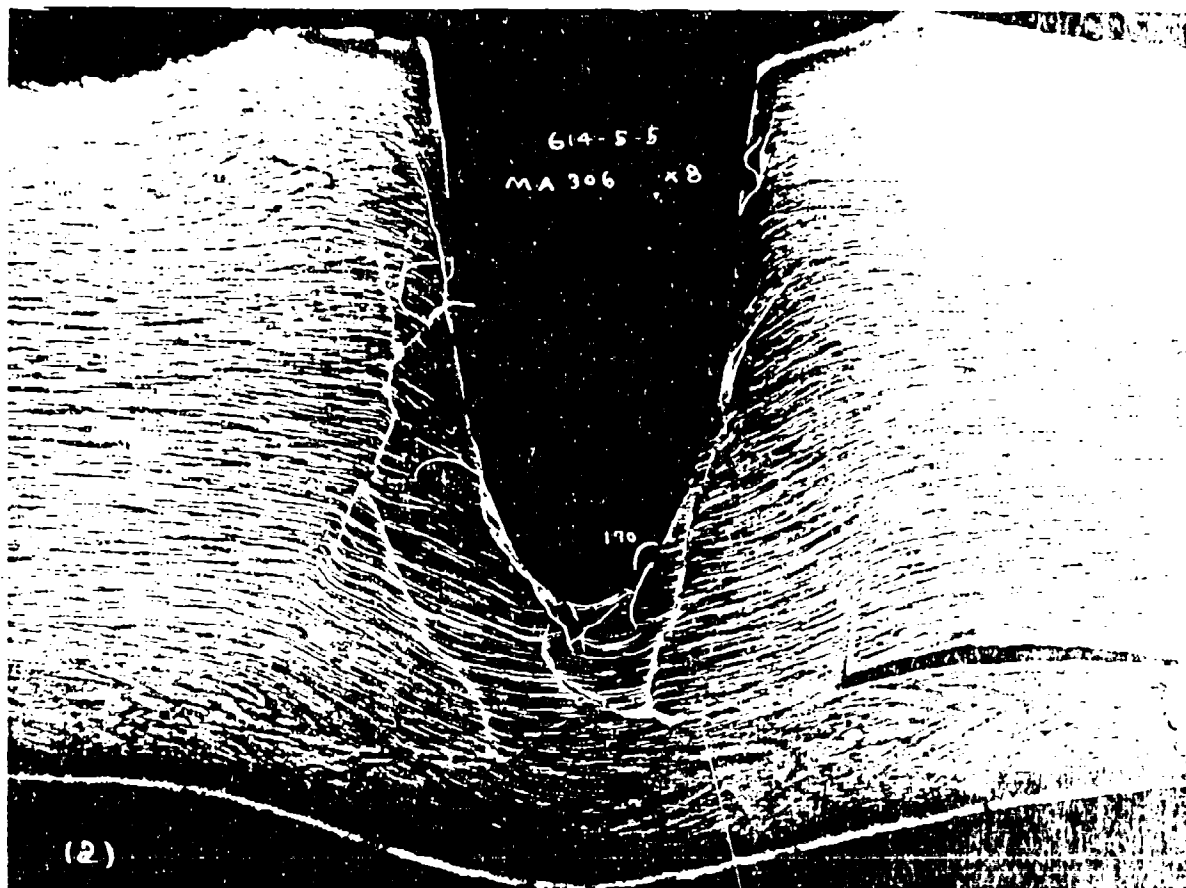
- (a) Shows cracking and slip of metal in a complete penetration of .30 caliber A.P. bullet into medium ballistic plate. This section is cut off-center from the axis of the bullet, and therefore appears to be only partial. Other penetrations in this plate buttoned badly, and in this macro study, the start of one is plainly shown.

#614-5 Round 5 - MA 306

- (b) Same plate as above, a partial penetration. Note another crack which, if propagated, would have caused a button.

#614-5 Round 8 - MA 380





Macroscopic examination of all samples indicate that there is a relation between the amount of "white layer" present and the ballistic resistance. To clarify, the greater the ballistic resistance, the greater the amount of "white layer". The progressive changes in the configuration of the "white layer" are shown in Figures 4 (a) to (e), which represent macrostructures of the same area after removing progressively from 0.02 to 0.05 inch of metal from each section. It is evident that the distribution and amount of "white layers" vary according to the position of the plane cut through the bullet hole.

A study of macrostructures thus shown illustrates a pronounced distortion of the banded structure about the bullet hole, indicating a flowing of the metal as it is forced aside by the bullet. It should be noted that the most severe and abrupt distortion of the banding occurs at the boundaries of the "white layer"; see Figures 2 (a), 2 (b), and 3 (a).

Figure 2 (a) illustrates a standard chromium-molybdenum-vanadium plate from which a button was blown off; early development of spalling on plates of this same composition is shown in Figures 3 (a), 3 (b) and 22 (f). The "potential" button cracks appear to have their origin in the bands.

Figure 4

Progressive changes in the configuration of the "white layer" are illustrated here. For each successive picture the specimen was re-surface ground and polished, which resulted each time in removing from 0.02 to 0.05" of metal from the surface. After each repolishing, the specimen was etched with a different etching reagent in order to determine which brought out the structure the best.

In these, as in the preceding photographs, a distortion of the banding about the bullet hole is very pronounced, indicating a "flowing" of the metal as it is forced aside by the bullet. It should be remarked that the most severe and abrupt distortion occurs at the boundaries of the "white layer".

Notice also the development of the three "white layers" branching from the tip of the crack so prominently in (e). In (a) they can be located by the deviation of the banding, but are certainly not recognizable as a layer, while in (b) they can be identified as a very thin layer of this peculiar structure.

- | | | |
|--|--------------|--------|
| (a) Etched with Oberhoffer's reagent | #WJ2-Round 3 | MA 237 |
| (b) Etched with Stead's reagent | | MA 278 |
| (c) Etched with Rosenhain & Haughton's reagent, diluted. | | MA 302 |
| (d) Etched with Humfrey's reagent | | MA 312 |
| (e) Etched with Dickenson's reagent | | MA 329 |

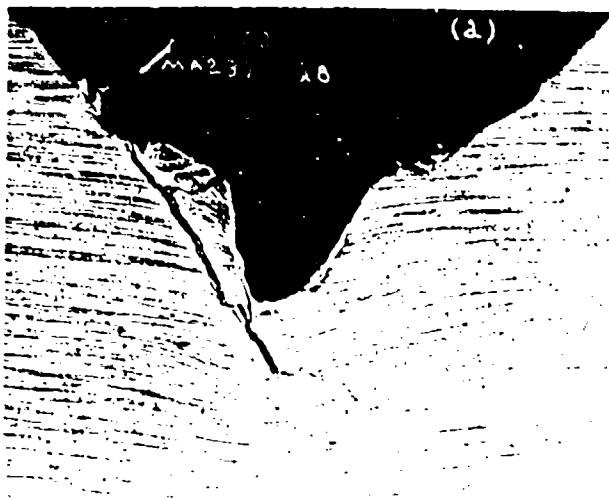
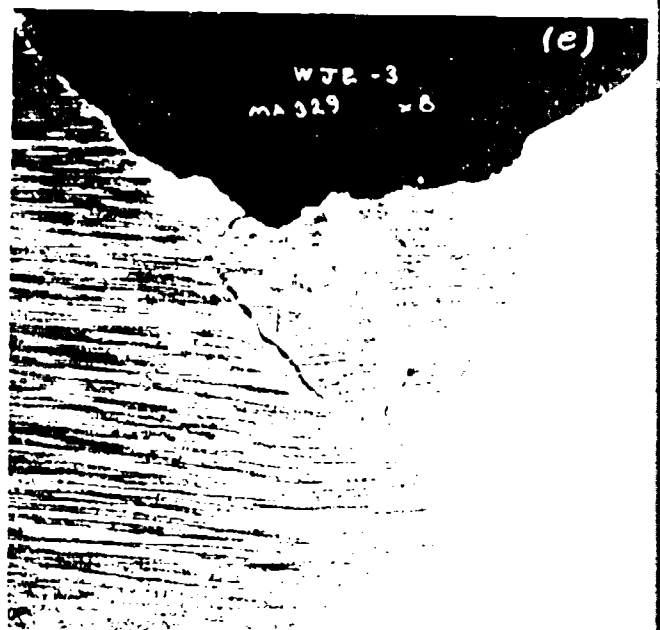
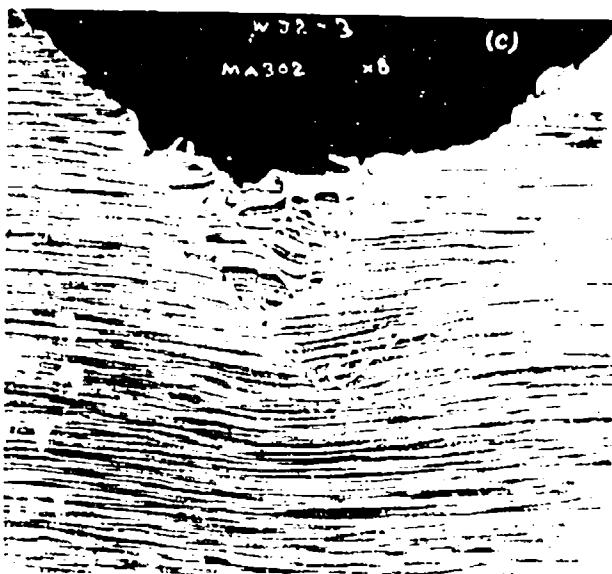
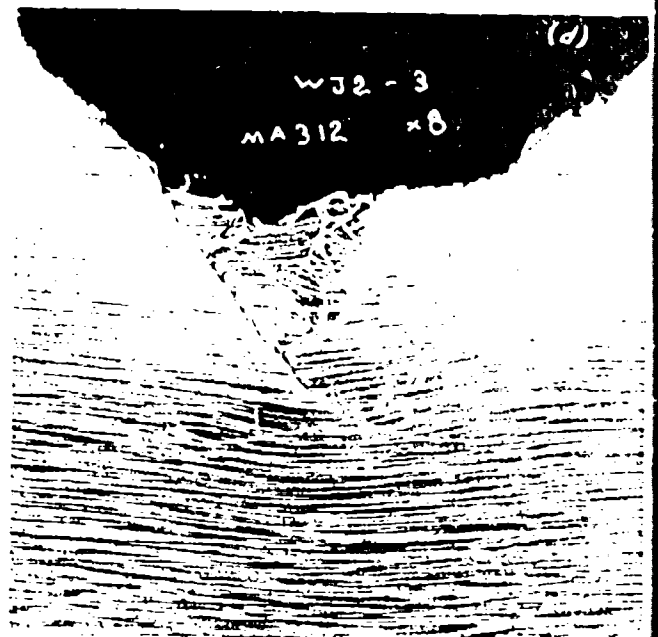
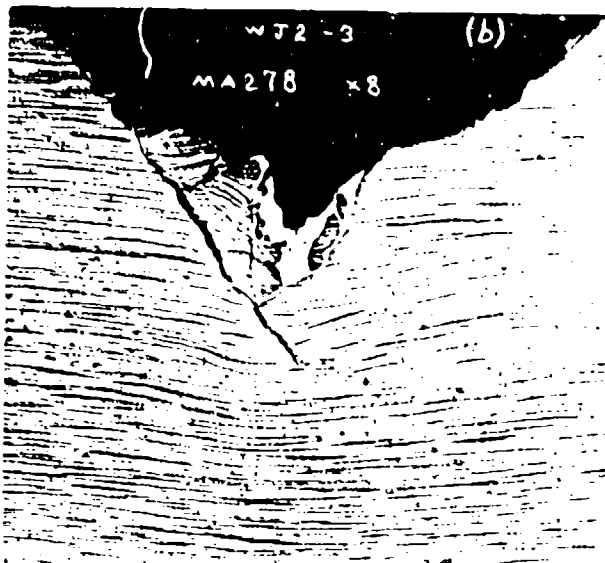


Figure 7

W 4 6 3 4 2 6



A macroscopic study was made on several sections of bullet holes cut parallel to the surface and removed by various amounts. A macro study of cross sections of bullet holes from the same plates has been discussed in the foregoing.

In the case of the plate WJ2, -4, containing 3.58% nickel and 2.01% silicon, which was partially penetrated, particles of plate were blown off at the entrance end of the plate, and therefore no distortion was evident on the surface layers, see Figure 5 (a). At a depth of approximately .166 inch below the entrance face of the plate, the first evidence of torsional flow of the metal as revealed by the swirling effect of the dendritic segregation is evident. Near the exit side of the plate, there is a decrease in size of area distorted by bullet impact.

Heavy membranes of "white layer" were present near the bullet hole in the layers near the entrance face of the plate. The orientation of these layers varied considerably. Crack systems were promoted by the severe twisting of the metal during bullet penetration. This plate is particularly interesting due to the fact that dendritic segregation persisted throughout the entire plate and evidence of the marked rotational effect of the bullet was revealed by the swirl of the dendritic segregation.

Figure 5

Plate #WJ2 - 4 High Ballistic Plate

Progressive changes in the macrostructure. Marked dendritic segregation persists throughout the layers as well as the torsional deformation caused by bullet spin.

- (a) Considerable metal blown out by the bullet, therefore no torsional deformation evident.

Rosenhain & Haughton etch. MA 345

- (b) Metal still blown out, slight swirl evident.

Oberhoffer's etch. MA 747

- (c) True picture of swirl evident since we are now below area blown out by bullet.

Oberhoffer's etch, as are all the following.

MA 772

- (d) " MA 806

- (e) " MA 853

- (f) Note deformation extends below the bullet hole.

MA 860

- (g) " " " MA 865

- (h) " " " MA 873

- (j) " " " MA 876

- (k) MA 886

- (l) Note crack forms at outer limit of swirl deformation. Corresponds to (c) above.

MA 773

- (m) MA 805

- (n) MA 854

- (o) Note the deformation extending below bullet hole.

MA 857

- (p) Note the deformation which, covering same area, shows less violent perturbation of metal.

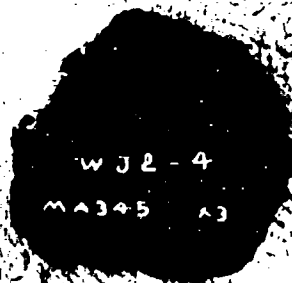
MA 866

- (q) MA 872

- (r) Note beginning of very slight decrease in area of disturbance.

MA 877

- (s) MA 885



X3

-a-

a- .337" ABOVE BOTTOM OF BULLET HOLE.



X3

-b-

b- .263" ABOVE BOTTOM OF BULLET HOLE.
FIGURE 5.

W.P. 651 677 H



X3

C - .191" ABOVE BOTTOM OF BULLET HOLE.

-C-



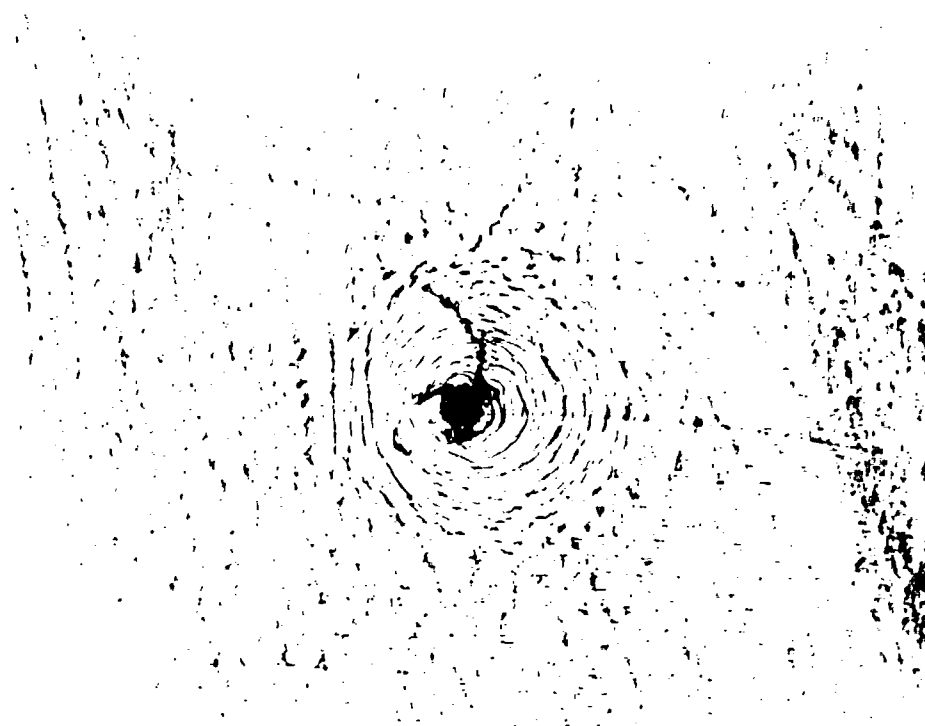
X3

d. - .126" ABOVE BOTTOM OF BULLET HOLE.

FIGURE 5.

-d-

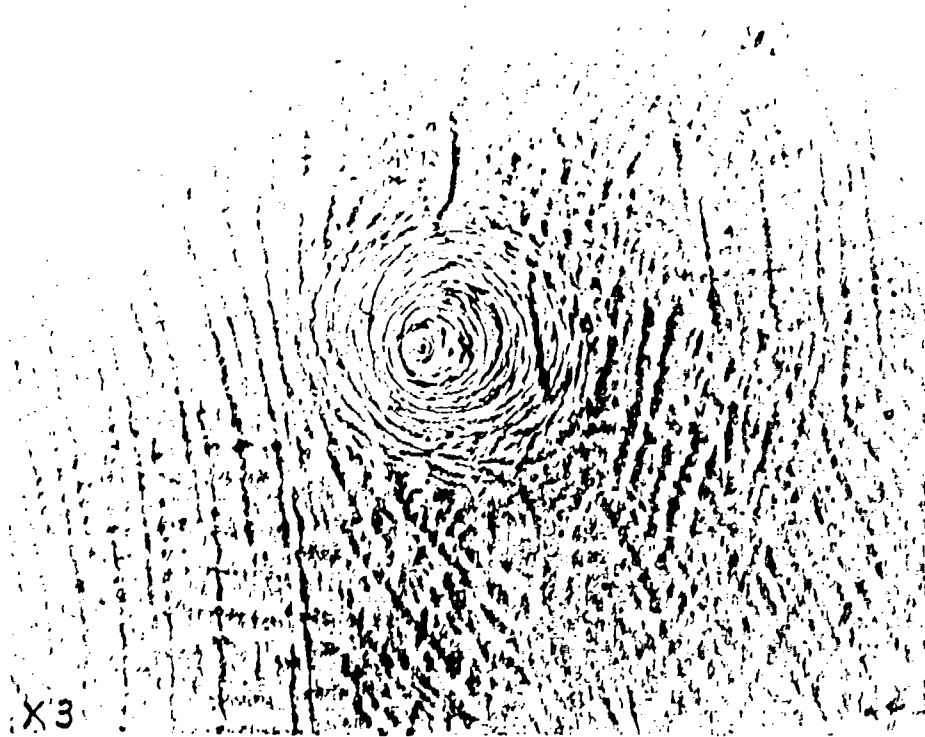
W.H. 631 677 12



X3

-e-

e. - .059" ABOVE BOTTOM OF BULLET HOLE.



X3

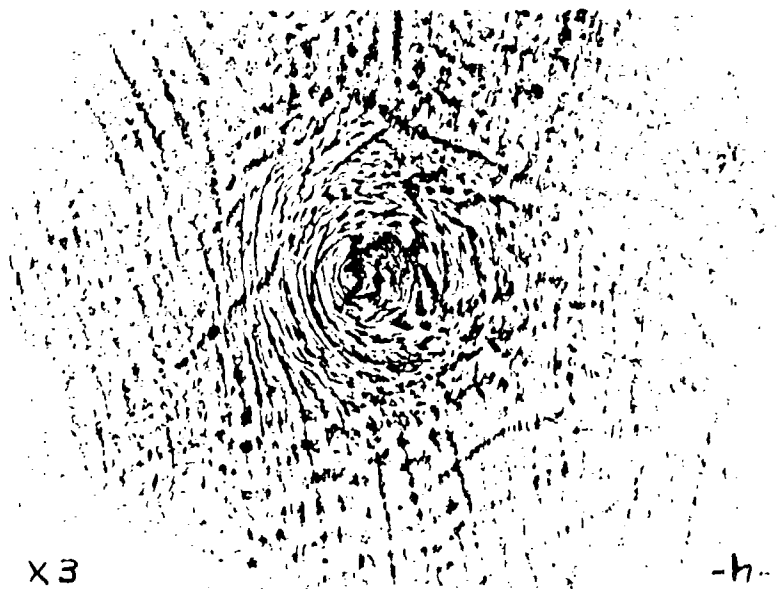
f - .005" BELOW BOTTOM OF BULLET HOLE.

FIGURE 3.

W. H. R. 6/7/71



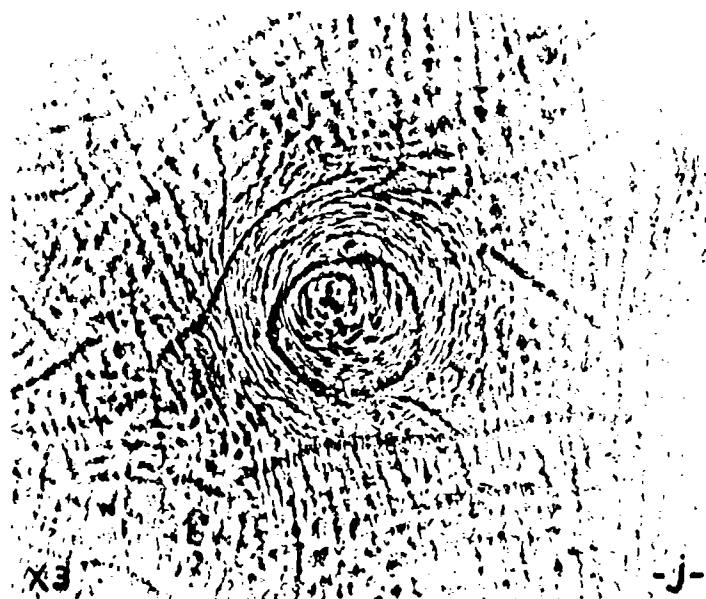
g - .015" BELOW BOTTOM OF BULLET HOLE



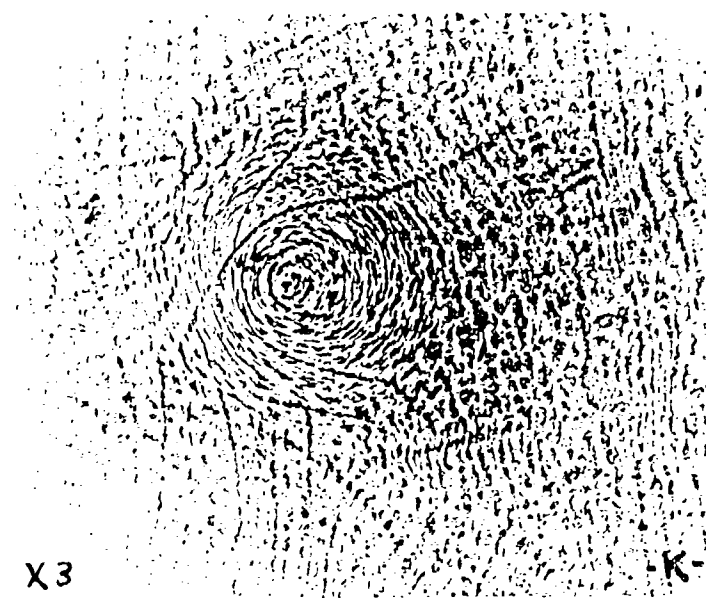
h. - .026" BELOW BOTTOM OF BULLET HOLE

FIGURE 5

W.D. 684 6271



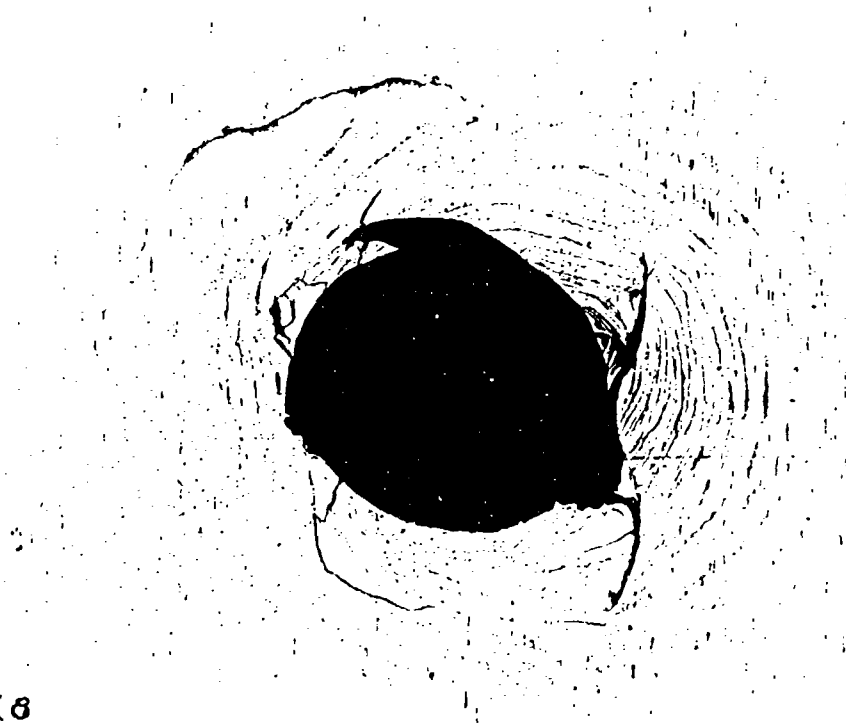
J. - .037" BELOW BOTTOM OF BULLET HOLE



K. - .048" BELOW BOTTOM OF BULLET HOLE

FIGURE 5.

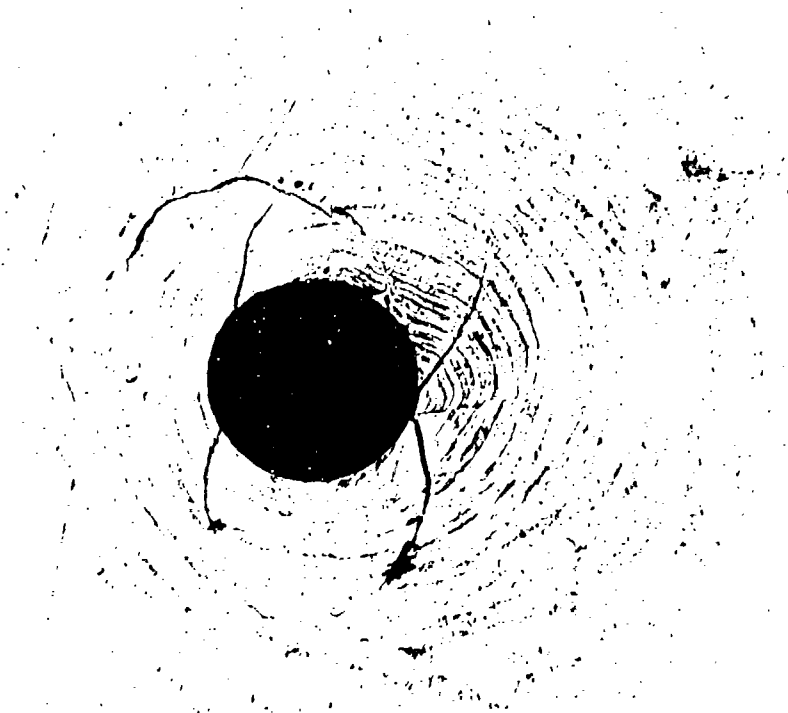
W.A. 639-677 E



X8

-l-

l. - .191" ABOVE BOTTOM OF BULLET HOLE.



X8

-m-

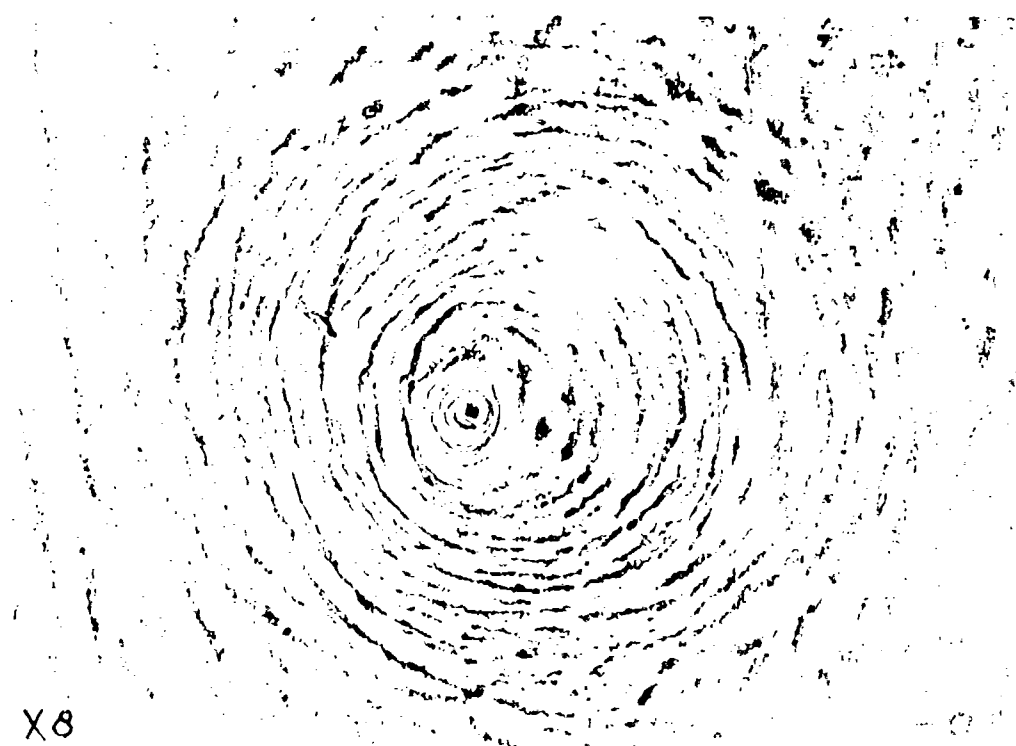
m. - .126" ABOVE BOTTOM OF BULLET HOLE.

FIGURE 5.

W 3 6 7 6 7

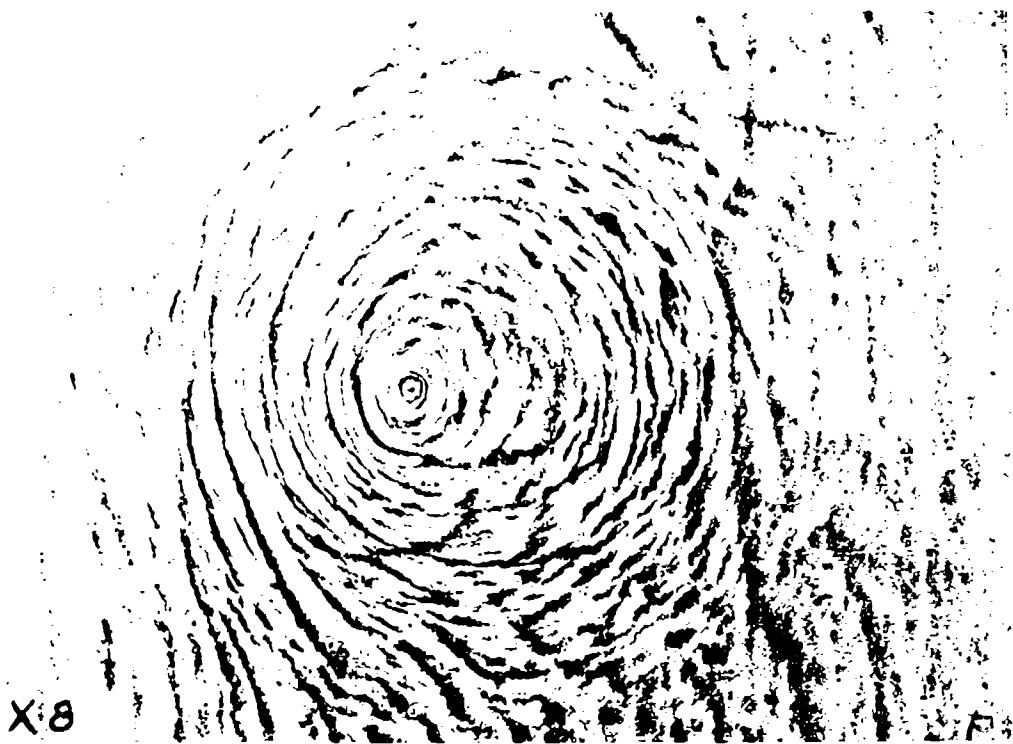


N. - .059" ABOVE BOTTOM OF BULLET HOLE



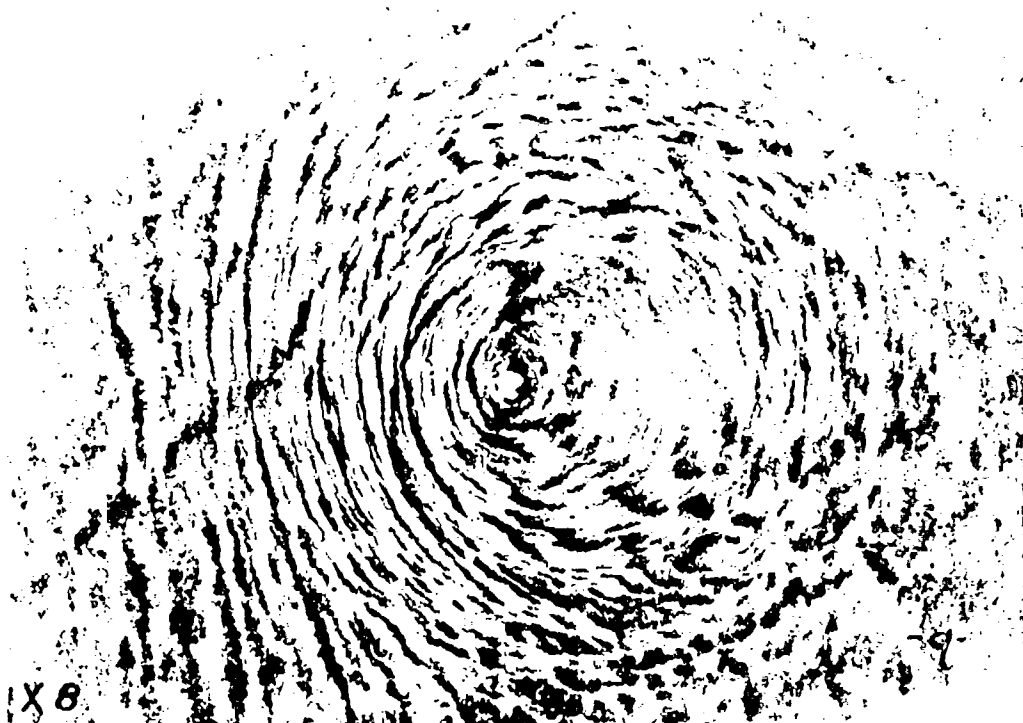
O. - .005" BELOW BOTTOM OF BULLET HOLE

FIGURE 3.



X8

p. - .015" BELOW BOTTOM OF BULLET HOLE.

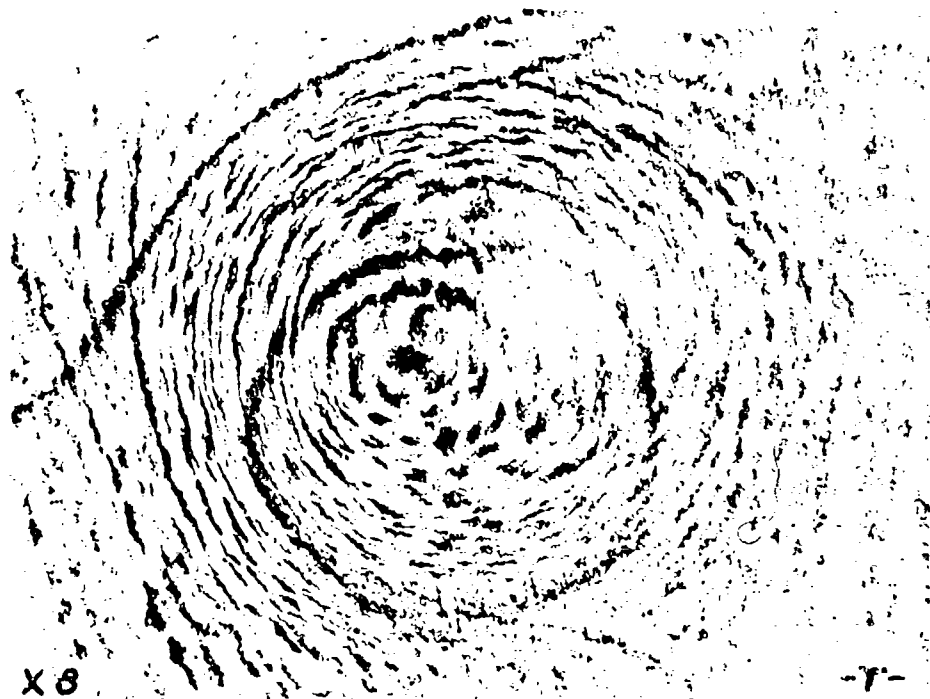


X8

q - .026" BELOW BOTTOM OF BULLET HOLE.

FIGURE 5.

W.A. 639-617 //



T. - .037" BELOW BOTTOM OF BULLET HOLE.



S. - .048" BELOW BOTTOM OF BULLET HOLE.

FIGURE 5.

W.A. 651 67 1

Figure 6

26-6 Medium Ballistic Plate

Consecutive layers through the surface show much the same sort of thing as Figure 5. However, the dendritic structure is almost negligible.

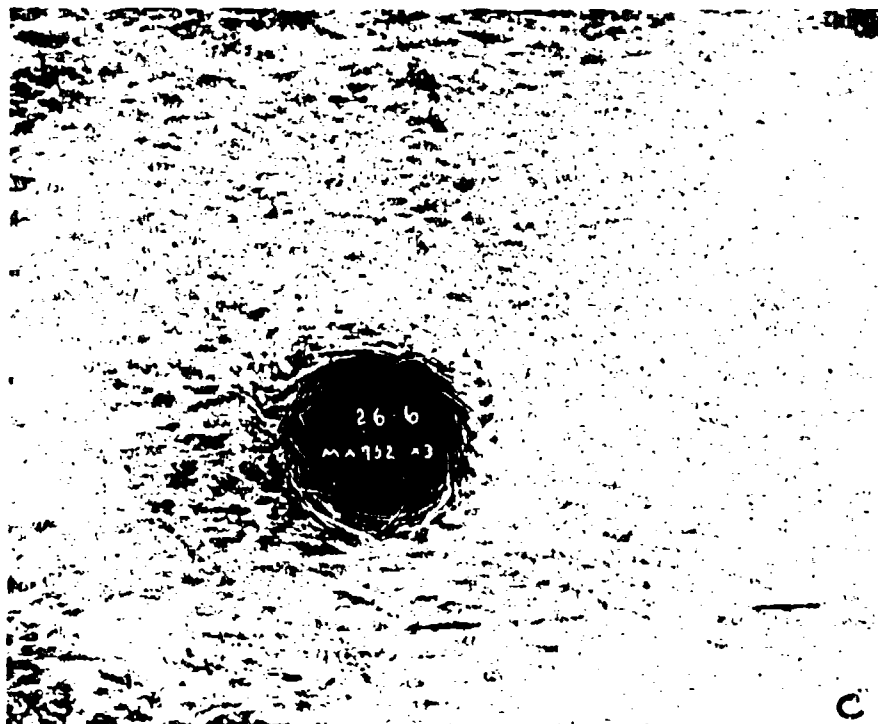
- (a) Blackened zone shows metal forced up by bullet impact. The light structureless body of the metal is the normal decarburized surface.
1% Nital MA 285
- (b) Swirling structure is slightly masked by the additional force introduced by the upheaval of metal. Oberhoffer's etch as well as the following.
MA 745
- (c) MA 752
- (d) Swirl of metal is undistorted MA 775
- (e) MA 803
- (f) MA 824
- (g) MA 874
- (h) Back face of plate. MA 855
- (j) Corresponds to (b) above. MA 746
- (k) MA 753
- (l) MA 774
- (m) MA 802
- (n) MA 825
- (o) MA 875
- (p) MA 856
- (q) Ball ammunition into armor plate. No swirling action of the metal about the edges of the bullet hole can be found.
Bullet: Cal .30 Ball M1, 2733 f.s. impact.
MA 813



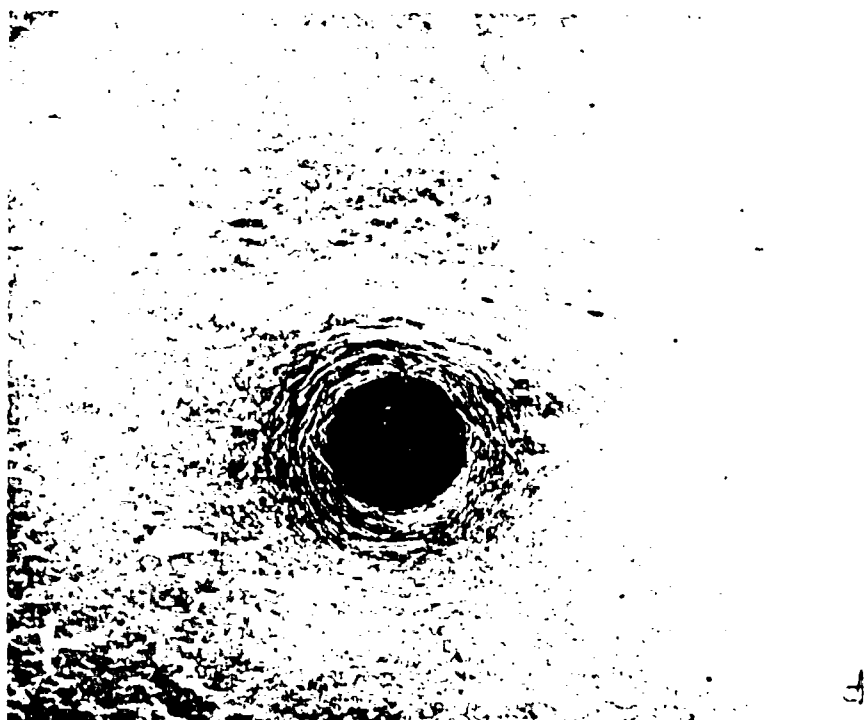
2



W.D. 657 6 8 9



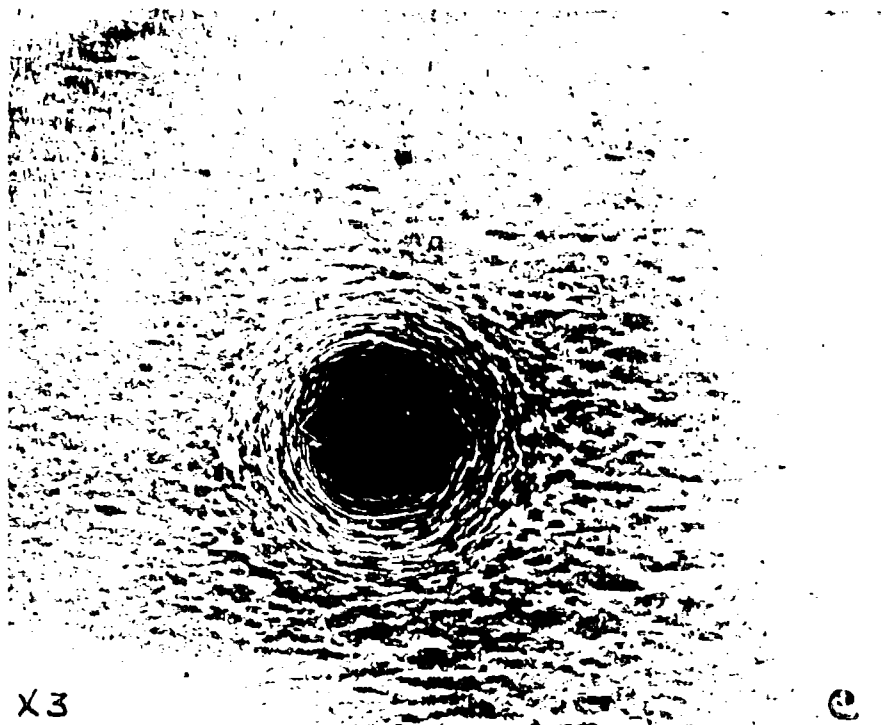
C. - .147" BELOW TOP OF ARMOR PLATE.



d. - .218" BELOW TOP OF ARMOR PLATE.

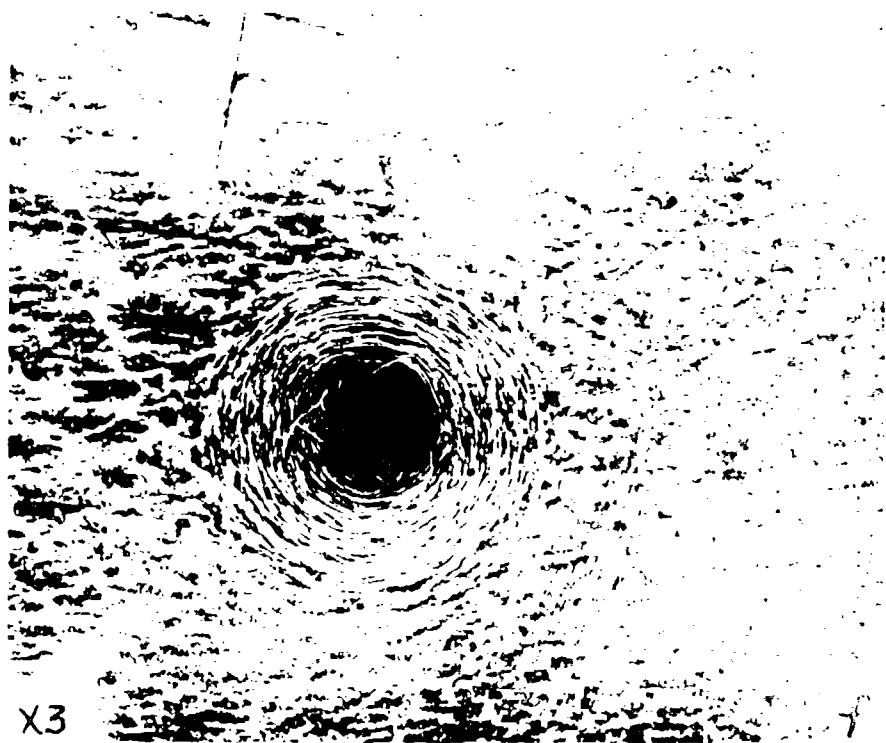
FIGURE 6

W.A. 639-678 B



X3

e. - .283" BELOW TOP OF ARMOR PLATE.

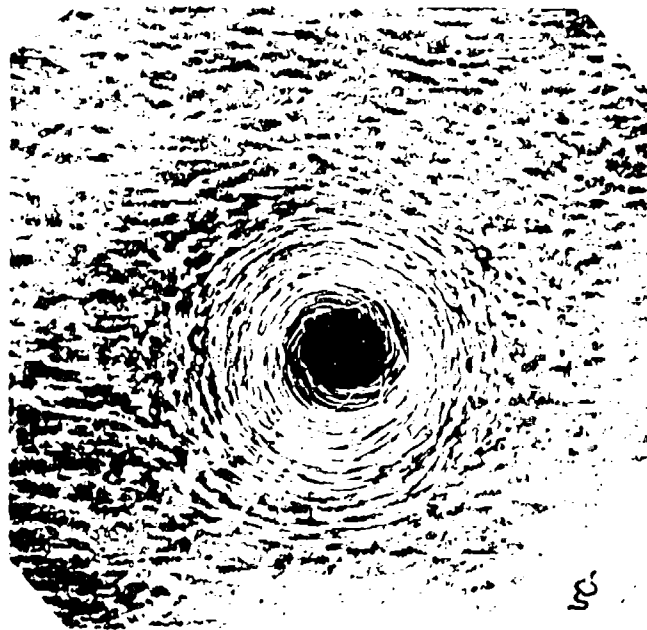


X3

f. - .364" BELOW TOP OF ARMOR PLATE.

FIGURE 6.

WHL 6-1-11



g. - .426" BELOW TOP OF ARMOR PLATE



X3

h. - .494" BELOW TOP OF ARMOR PLATE.
.008" ABOVE BOTTOM OF PLATE.

FIGURE 6.

W. H. E. 100



X8

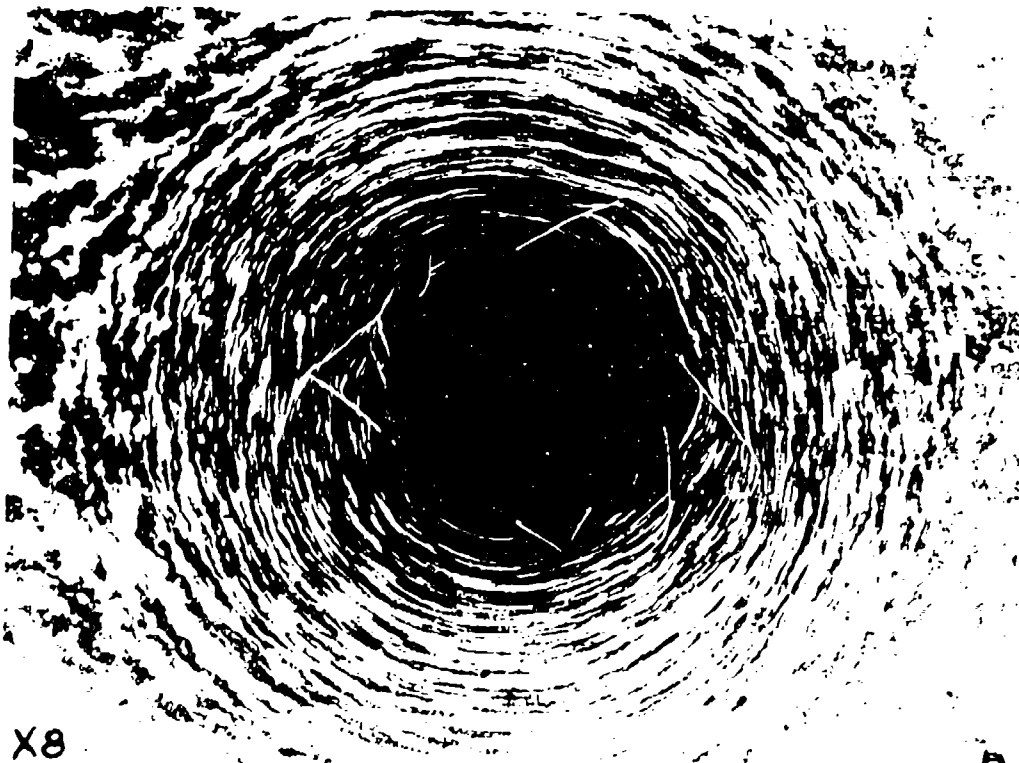
J - .613" BELOW TOP OF ARMOR PLATE.



K - .197" BELOW TOP OF ARMOR PLATE.

FIGURE 6.

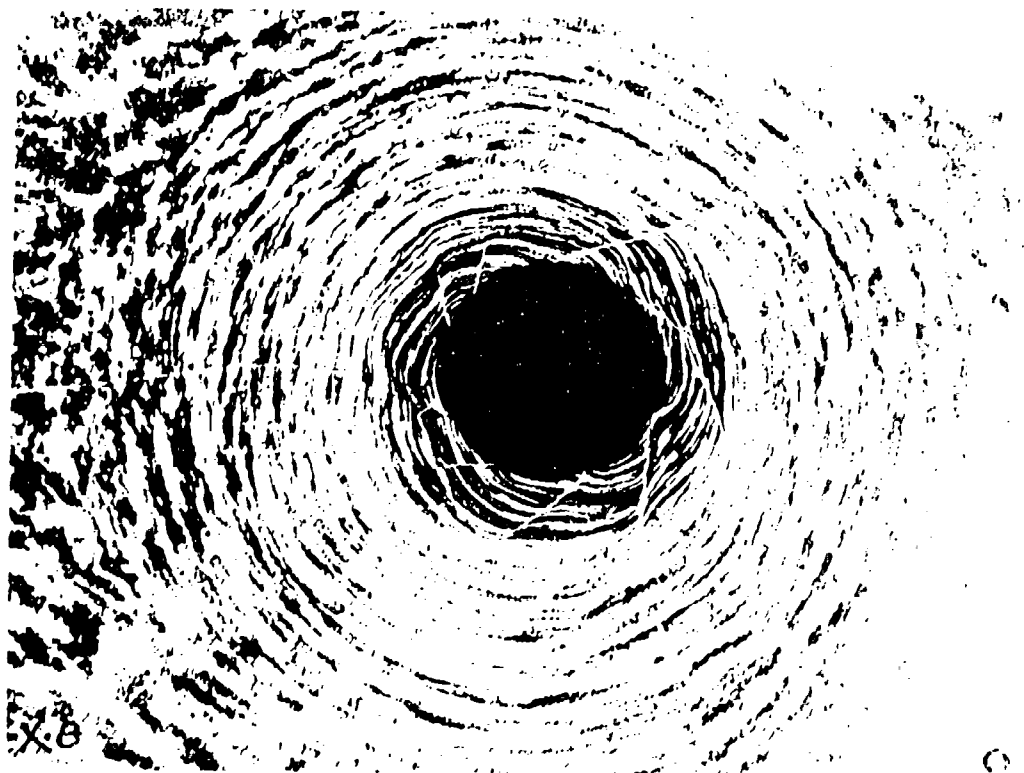
10-6-11-2



X8

N. - .364" BELOW TOP OF ARMOR PLATE.

n
X8

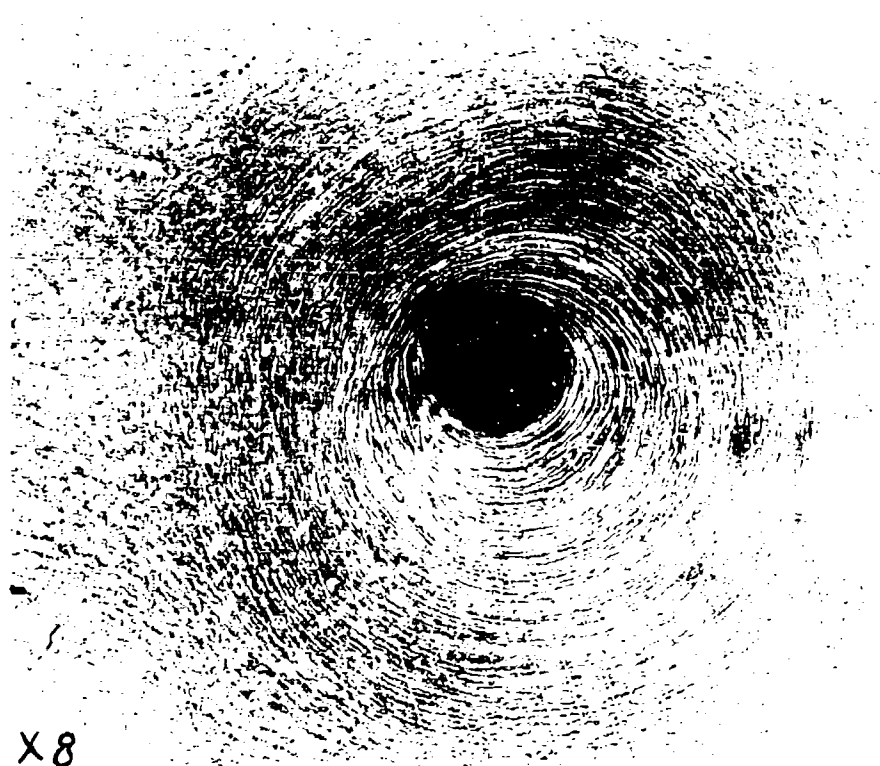


X8

O. - .426" BELOW TOP OF ARMOR PLATE.

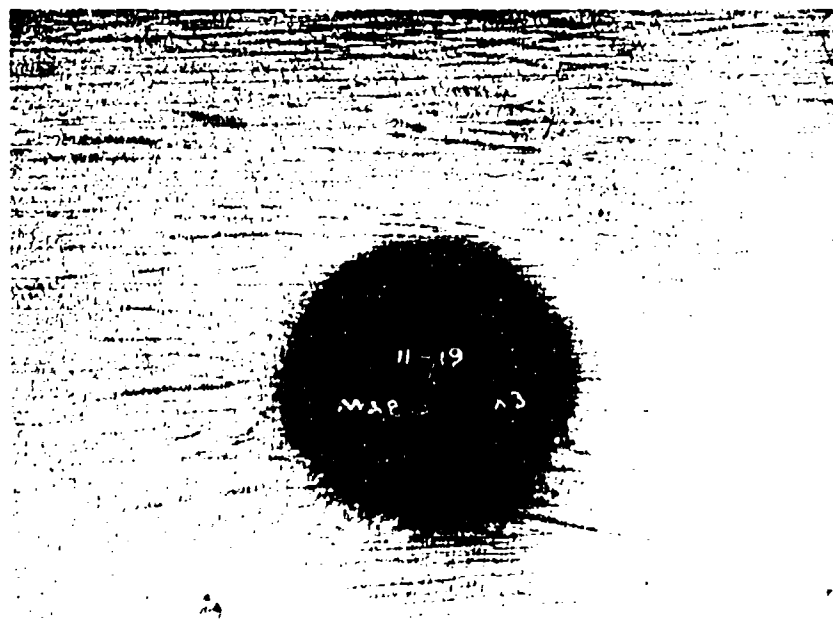
FIGURE 6.

10-11-65



X8

P. - .494" BELOW TOP OF ARMOR PLATE.
.008" ABOVE BOTTOM OF PLATE.



X3

q. - .015" BELOW TOP OF ARMOR PLATE.
CAL. 30 BALL - M1 - PENETRATION IN
ARMOR PLATE.

FIGURE 6
W.D. 635-675 H

Figure 7 (a) illustrates graphically the contour of the area disturbed and twisted by the bullet.

Figure 6 illustrates the progressive changes in macrostructures of area affected by bullet impact in a standard chromium-molybdenum-vanadium plate completely penetrated by a Cal .30 A.P. M1922 bullet.

In the first three layers, the outer portion of the swirl is masked by the upheaval of the metal forced back by the bullet.

This upheaval of metal is clearly revealed in 6 (a).

Beginning at and extending below the ogive to a depth of 0.35 to 0.45 inch, a decided twist is evident and then it decreases in intensity at the exit face of the plate.

Since the force causing the twisting of the metal has the same direction as the spin of the bullet, it is reasonable to assume that this distortion is produced by the bullet spin.

A study of the macrostructures of this series indicates that "white layers" represent planes of greatest slip stress, oriented 30 to 45 degrees to direction of impact, and persist at the bullet hole. A circular swirl of deformed dendritic segregation as the result of the spinning of the bullet was clearly evident.

Figure 7 (b) illustrates the hour glass shaped contour of the area affected by bullet impact.

PLATE NO. WJR
PENETRATION NO. 11.

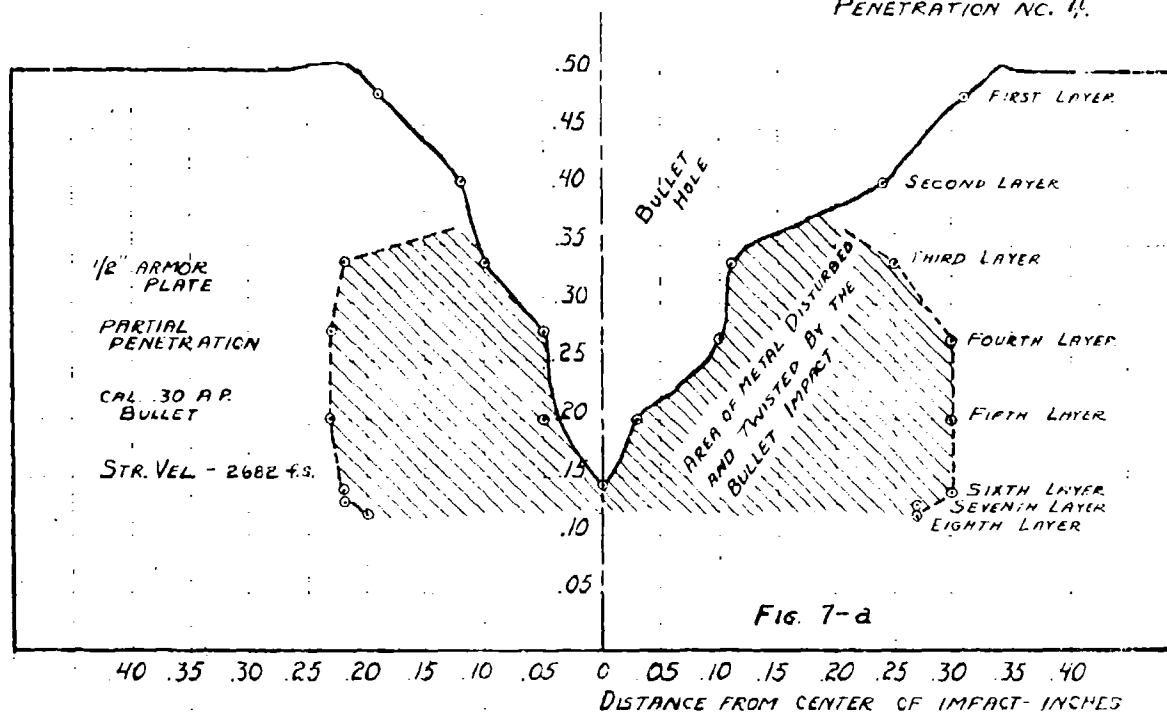


PLATE NO. EX 26
PENETRATION NO. 6.

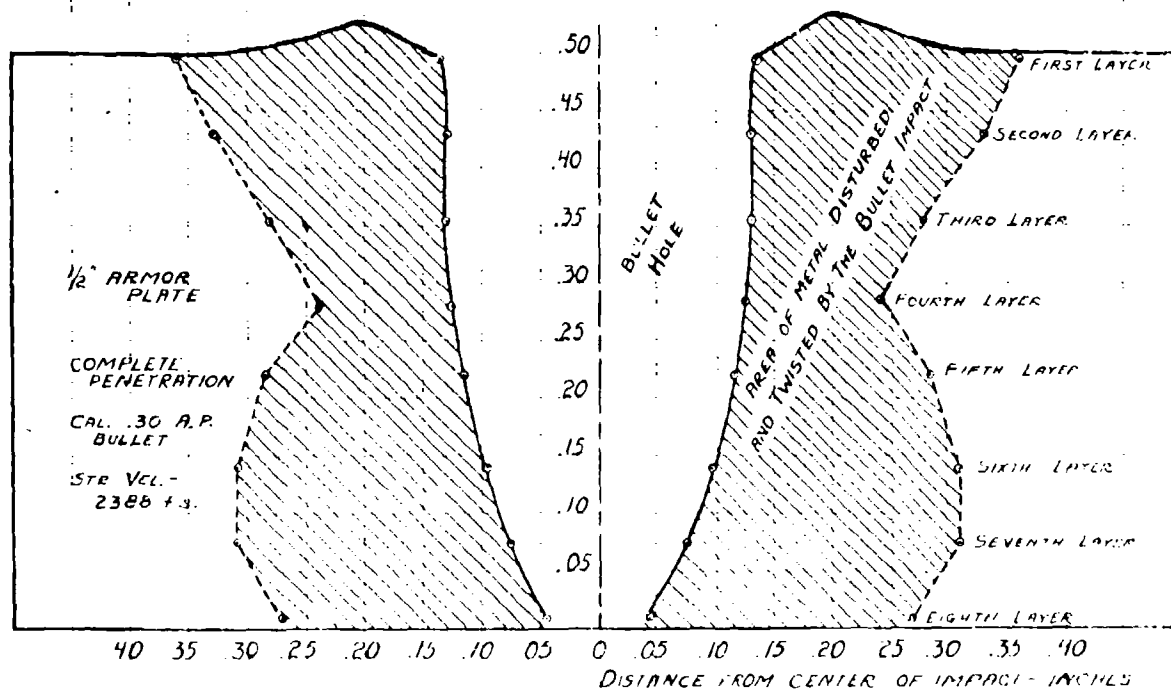


Figure 8

- (a) Twisting of metal inside hole made by armor piercing bullet impact. Unetched.

MA 832

- (b) Scale blown off back of armor plate by bullet impact shows characteristic Läder line pattern. See Figures 9 (a) & (b). Unetched.

710-200

It is interesting to note the similarity of the hour glass shaped contour of the area in armor plate of the standard composition and a similar strained area revealed by Fry's reagent around a partial penetration in a low carbon steel plate.

To confirm the opinion that the twisting of plate metal about the bullet hole was caused by the spin of the bullet, there is illustrated (Fig. 6 (q)) a punching impact made with ball ammunition. Due to the flattening of the lead immediately on striking, no spinning action was introduced into the plate, and true to predictions, no torsional flow could be found in this plate.

Spiral striations on bullet cores as the result of a boring action through plate are shown in Figure 8 (c).

Twisting of the plate metal when an armor piercing bullet strikes armor plate is clearly shown in Figure 8 (a).

Strain markings in the form of Lüder lines are occasionally revealed on the rear face of armor plates due to the fact that scale is sometimes blown off in these formations, see Figures 8 (b)

This scale pattern has no obvious relation to the occurrence of "white layer".

It has been impossible thus far to reveal strain markings or Lüder lines in armor plate by various methods of etching. Fry's reagent, which is recommended for

Figure 8

- (a) Twisting of metal inside hole made by armor piercing bullet impact. Unetched.

MA 832

- (b) Scale blown off back of armor plate by bullet impact shows characteristic Lüder line pattern. See Figures 9 (a) & (b). Unetched.

710-200

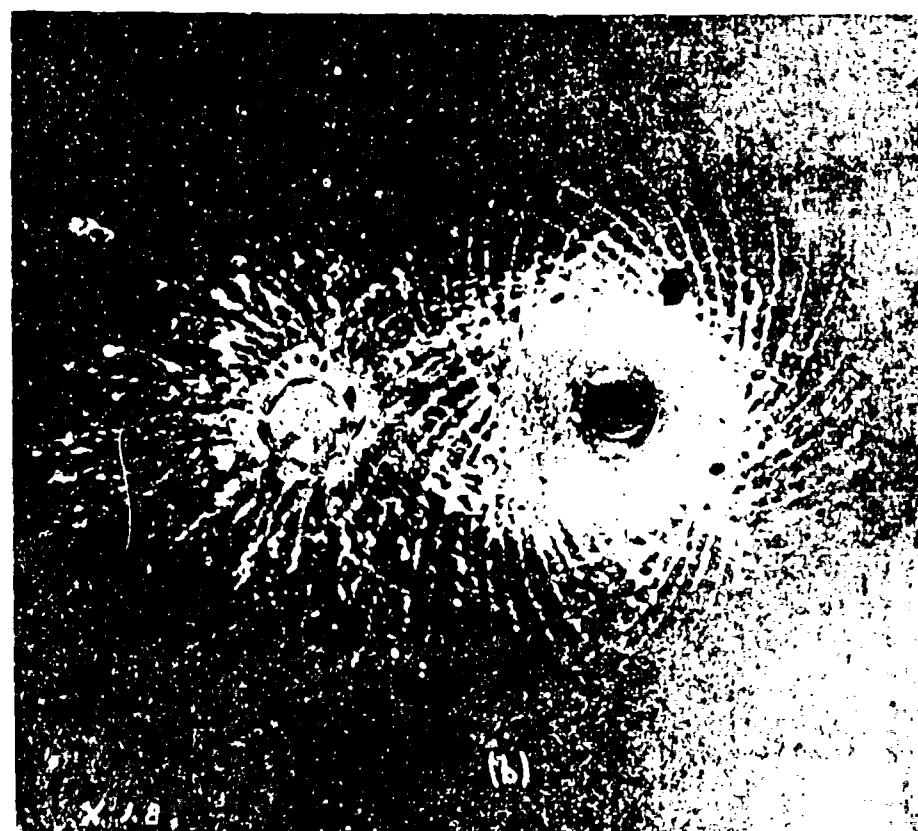
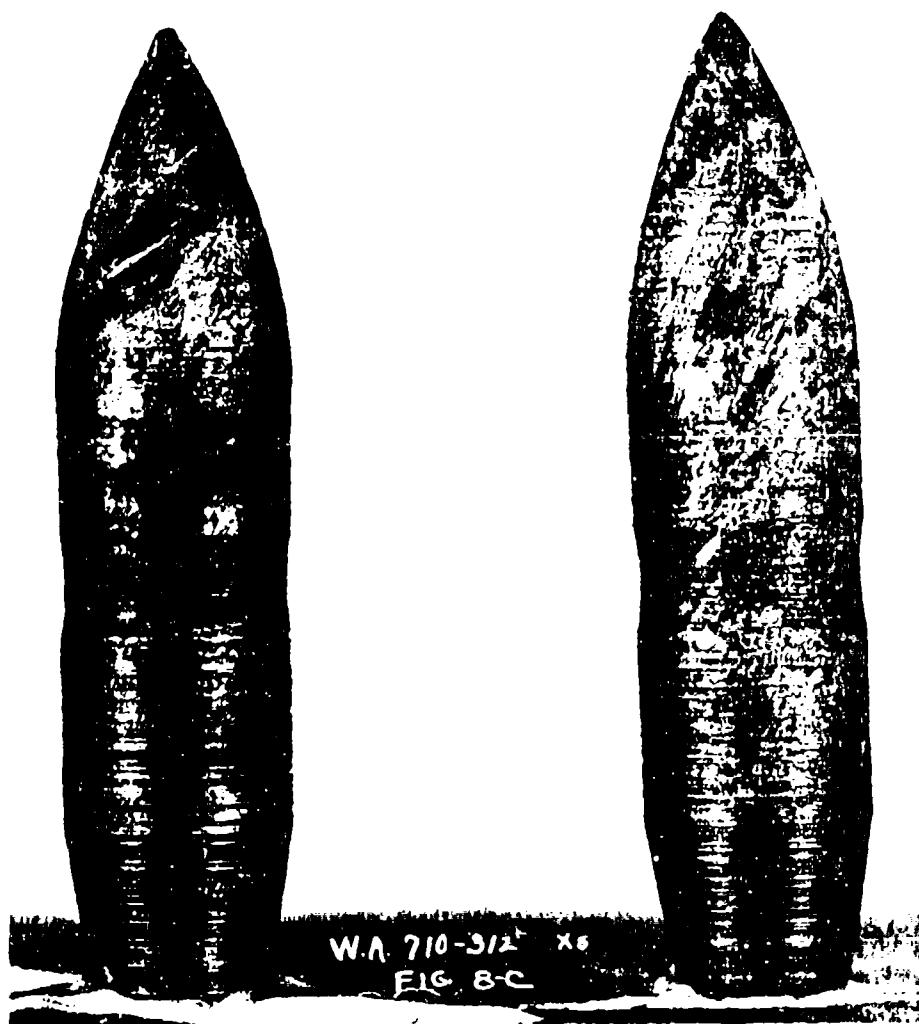


FIGURE 8.



revealing strain in low and medium carbon steels, is not suitable for revealing strain in armor plate, due to the fact that no free ferrite persists in heat treated armor plate. There are inserted photographs, Figures 9 (a), (b), which illustrate clearly Lder lines on the front and back faces of a low carbon steel plate subjected to impact with Cal .30 ball ammunition at a striking velocity of 2600 f.s.

It is interesting to note that Lders on the rear face of low carbon steel plate affected by bullet impact, as revealed by the Fry reagent, are quite similar to the strain markings on the rear face of the same plate shown by blowing off scale, see Figure 8 (c).

Microstructure

Normal etching reveals clearly the movement or faulting of the metal near the bullet hole but, on the other hand, fails to reveal the internal structure of the "white layer", as shown in Figure 10 (a), (b) and (c). The abrupt shift in the banding continuity from one side of the "white layer" to the other in Figures 10 (a) and (b), shows distinct evidence of a sudden slipping of the metal in the plane through the layer. The degree of this deformation is evident when it is considered that in the undistorted region beyond the bullet hole, the banding is perpendicular to the direction

Figure 9

- (a) Lüder lines on face of low carbon plate
after impact with ball ammunition
2600 f.s.

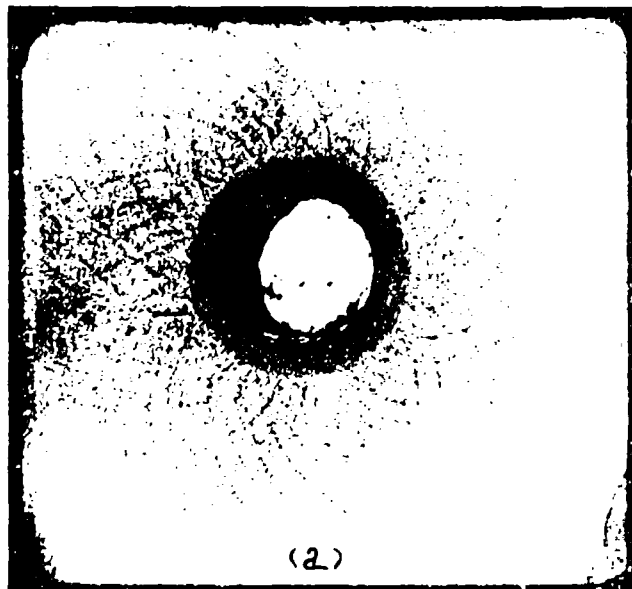
Fry's reagent after heating 45 minutes,
preheating at 200°C.

MA 823

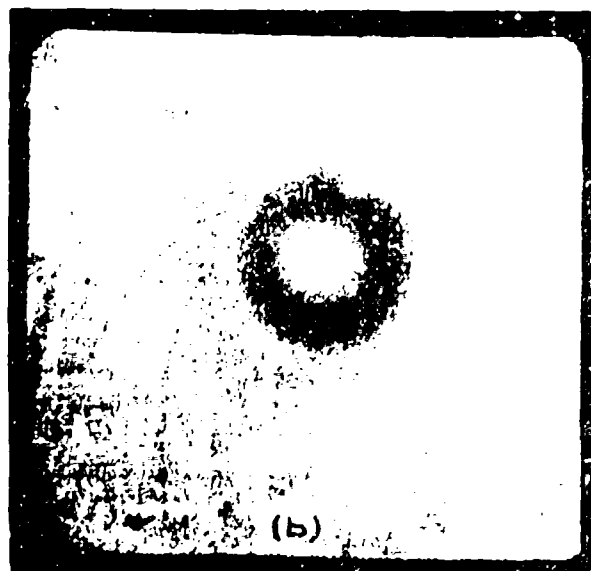
- (b) Rear face of same plate.

Fry's reagent after heating 45 minutes,
preheating at 200°C.

MA 871



a. - .085" BELOW TOP OF PLATE.



b. - .492" BELOW TOP OF PLATE.
.091" BELOW BOTTOM OF HOLE.

FIGURE 2.

WELDED

Figure 9 (c)

Scale blown off back of low carbon plate subjected to A.P. bullet impact of various striking velocities. Scale blown off back of plate shows characteristic Lüder line patterns.

710-182

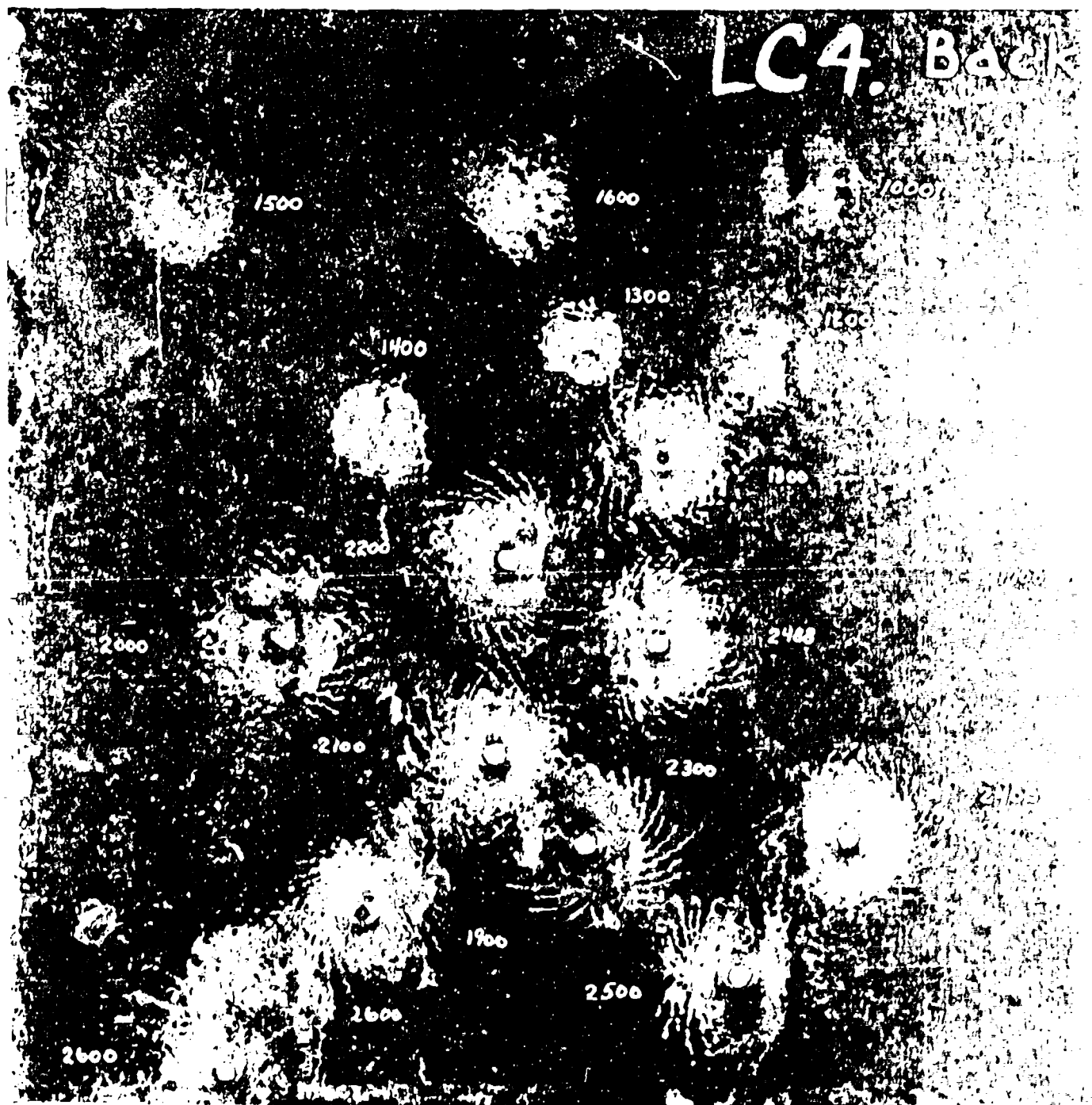


FIGURE 9. C.

Figure 10

- (a) The abrupt shift in the banding continuity from one side of the layer to the other shows distinct evidence of a sudden slipping of the metal in the plane thru the layer. The degree of this deformation is seen when one considers that in the undistorted region beyond the bullet hole, the bands are perpendicular to the direction taken by the bullet, whereas here they are off this normal by approximately 60°. The pronounced drawing in of the metal toward the tip of the layer occurs in almost every case.

1% Nital #Ex 26 Round 5. MA 175

- (b) The macroetch does not define the banding so clearly as the others but the slipping of the metal, as well as the change in direction of the banding across this peculiarly shaped boundary, is evident. The path of this layer does not follow any apparent rule, and this one case illustrates typical behavior, (not in shape, but in the apparent irregularity of path), of a considerable proportion of the layers.

Rosenhain & Haughton's reagent. #614-5 Round 5c
MA 412

- (c) In this case the layer seems to be the boundary of an angular deflection of the banding, rather than the place of a linear shift in their continuity. The "density" of these bandings also appears different on each side, showing a kind of compression of the banding on the side nearest the bullet hole. 1% Nital, #Ex 26-Round 5 MA 175

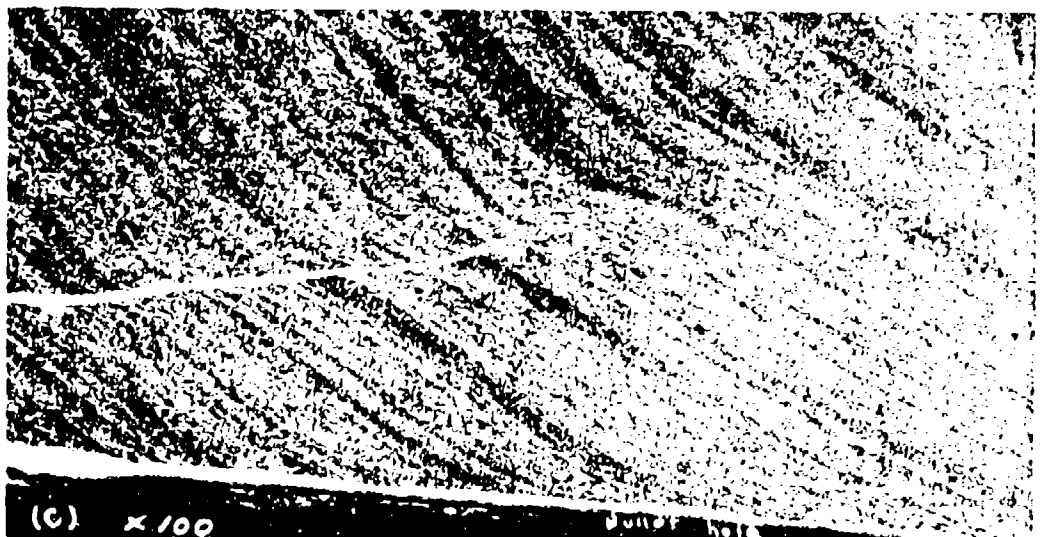
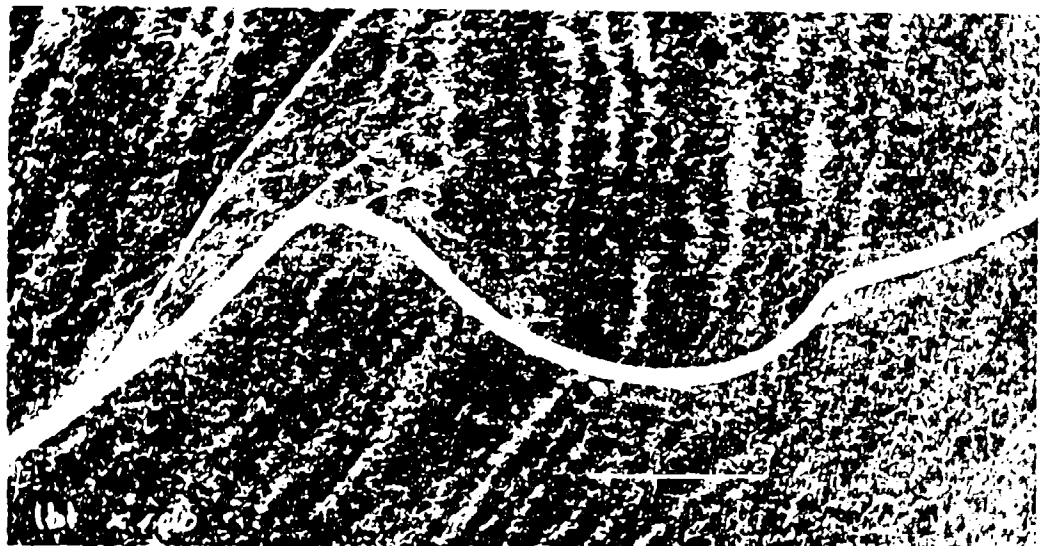


FIG 10

W.H. (57) 482

taken by the bullet, whereas in the cases illustrated they are deflected from 45 to 60 degrees from normal.

The "white layers" which are shown in Figures 10 (a), (b), and (c), and in 12 (c) and (d) are typical of those examined in various armor plate compositions, and it is evident that they are not oriented in any particular direction with respect to the axis of the bullet. They occur either parallel to or at various angles to the bullet axis, see Figures 11 (a), 11 (c), 12 (c), (d), 13 (a) and (b).

It was determined that "white layers" were present occasionally at the edges of the bullet hole, as shown in Figures 11 (a) and 20 (a). It is interesting to note that these particular "white layers" are etched more readily than those away from the bullet hole. Typical flow lines are evident in the layer at the edge of the bullet hole, Figures 11 (a), and 12 (a).

In the case of some "white layers" close to the bullet hole, flow lines are present in the outer borders of the layer, see Figure 11 (b). Also, after a relatively deep etching, a coring effect is noted in some of these "white layers", see Figures 11 (b), (c) and 12 (b). It is possible that the heat of bullet impact has tempered some of the "white layers", thus producing troostitic borders (softer material).

Figure 11

- (a) Illustrating the sort of fine "flow" lines found at the outer edges of many of the broader layers. Here they branch into a relatively thick layer which forms a coating on the bullet hole, where they become more pronounced. A coating like this, which shows the "flow lines so plainly in all cases, etches much more readily than layers in the interior of the metal, regardless of whether "flow" lines are found or not.

1% Nital #614-5 Round 5 MA 170

- (b) Etching to the extent shown in this micrograph, which brings out a set of "flow" lines to a considerable depth into the layer, was rarely found on a lightly etched and untempered specimen. The layer is also unusually broad.

1% Nital #614-5 Round 10, MA 399

- (c) Layer which runs quite parallel to the bullet hole. Notice here also the "coring" effect caused by the partial etching of the borders while the center remains unetched.

1% Nital #614-5 Round 3 MA 164

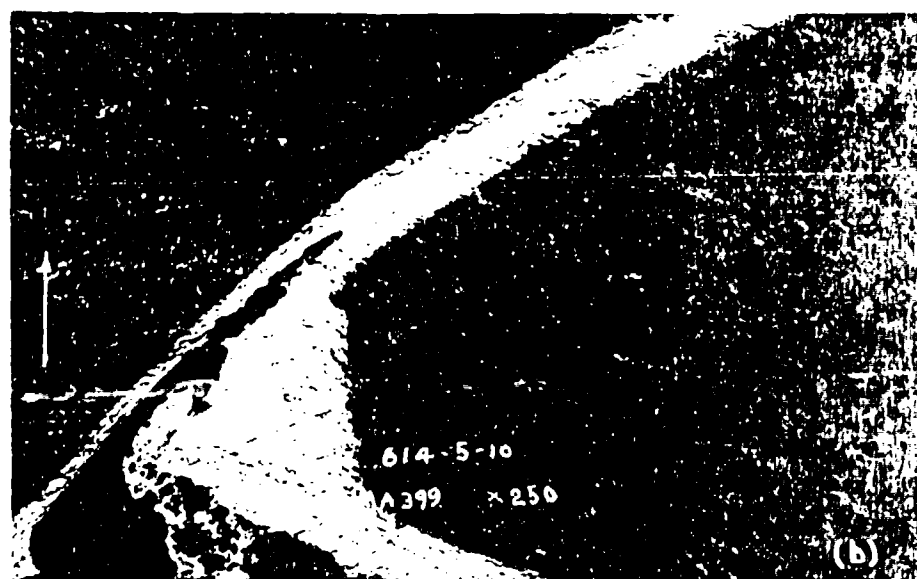
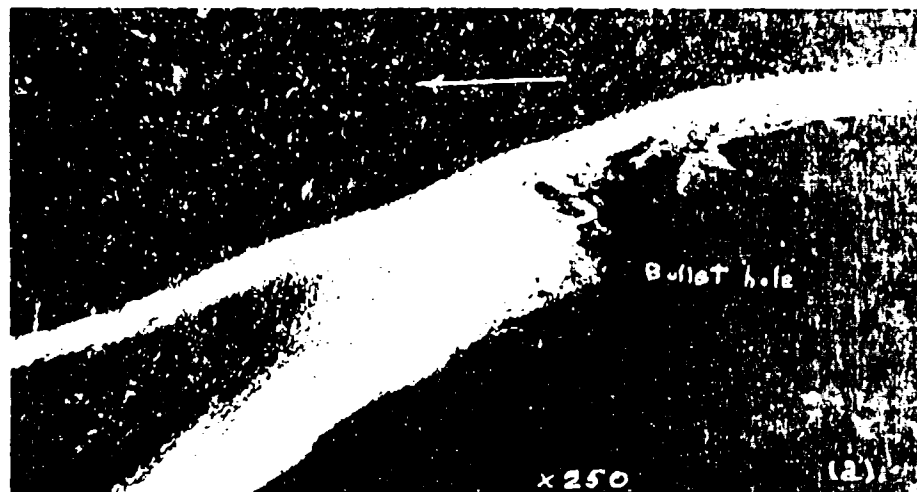


FIG. 11

W A 637 683

Figure 12

- (a) Deformed metal at lower edge of the penetration cavity. Usually the "white layers" at the edge of the bullet holes are readily etched as shown in this photomicrograph.

2% Nital #614-5 Round 8 HAL-101

- (b) Coring effect at edge of "white layer". This coring effect is probably caused by tempering of the martensitic "white layer" as the result of heat from bullet impact, thus producing troostitic borders.

5% Nital #614-5 Round 8 HAL-140

- (c) Layer branching out at 45° angle from bullet hole.

1% Nital #614-5 Round 9 MA 172

- (d) This "white layer" which terminates in the vicinity of much slag, does not seem to have any relation to it.

1% Nital #614-5 Round 10 MA 398

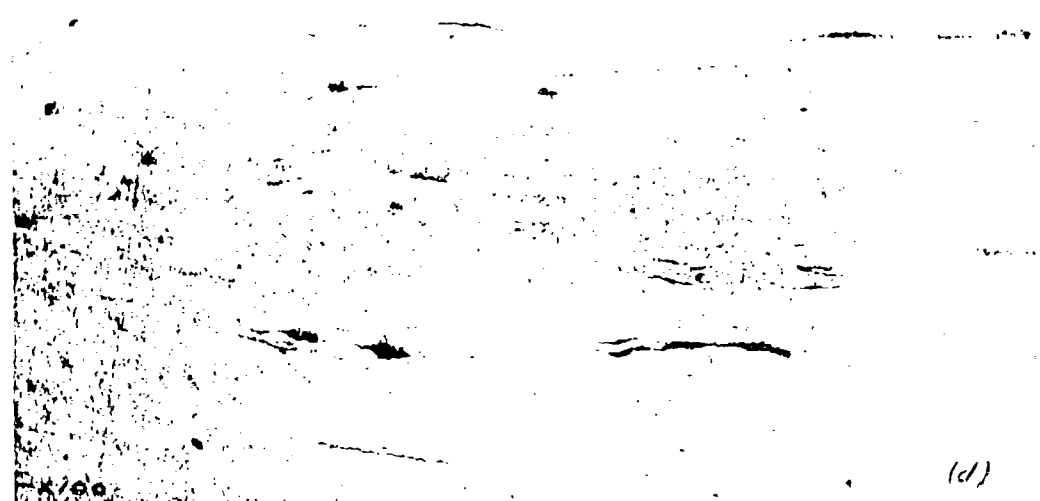
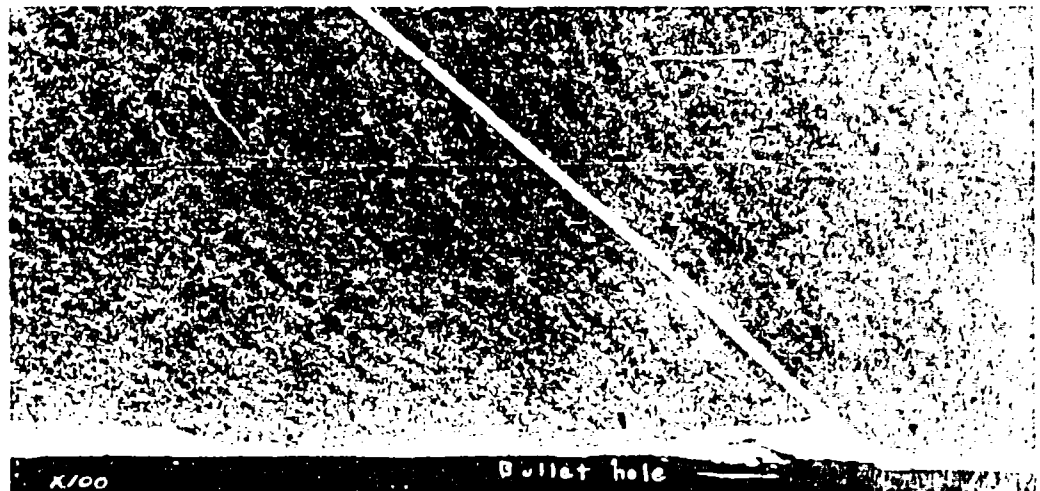
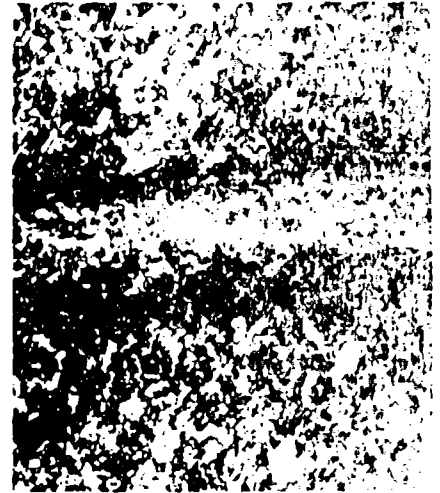
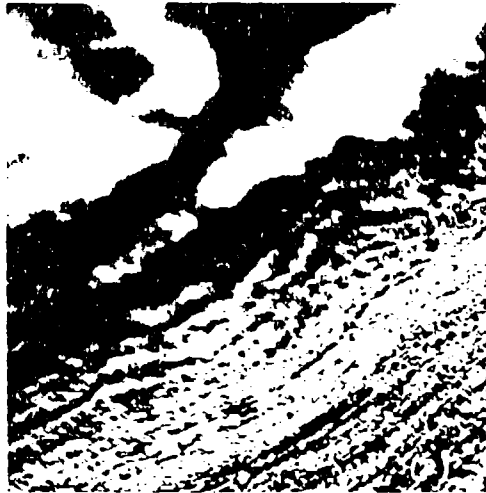


FIG 12

WA 639 684

On one occasion it was determined that after a "white layer" was formed, the metal slipped along a plane which was clearly revealed by etching, see Figure 14 (a).

"White layers" do not follow nonmetallic inclusions of the stringer type, as shown in Figures 12 (d) and 16 (d).

It has been shown under high power examination that rounded nonmetallics are present in the "white layers", in contrast to deformed or broken nonmetallic inclusions outside the "white layer", see Figure 15 (c).

On the other hand, Figures 15 (a) and (b) show unaffected nonmetallics adjacent to and partially within the "white layer".

It was difficult to correlate the formation of crack systems with "white layer" formation. Basing a conclusion on the direction and occurrence of cracks in relation to the "white layers", they may be divided into two classes:

- (a) Cracks which may have formed during the formation of "white layer", Figures 16 (a) and (b), 14 (c) and (d), 17 (a), (b), and (c);
- (b) Cracks which may have formed after the layer, Figures 11 (b) and 13 (a);

In nearly one-third of the "white layers" examined, crack systems were found showing evidence of twisting, or rupture by tearing the metal apart, Figures 16 (b), 17 (a), (b) and (c).

Figure 13

- (a) An interesting concurrence of crack and "white layer", although no inference can be drawn as to any inter-relation of the two.

1% Nital #614-5 Round 10. MA 400

- (b) This shows an abrupt shift in the crack's continuity at the boundary of the "white layer", indicating either a slipping of this whole layer after the formation of the crack, or a slipping of the metal after the crack's formation that was part of the process of layer formation.

1% Nital #A Carburetor Cover MA 229

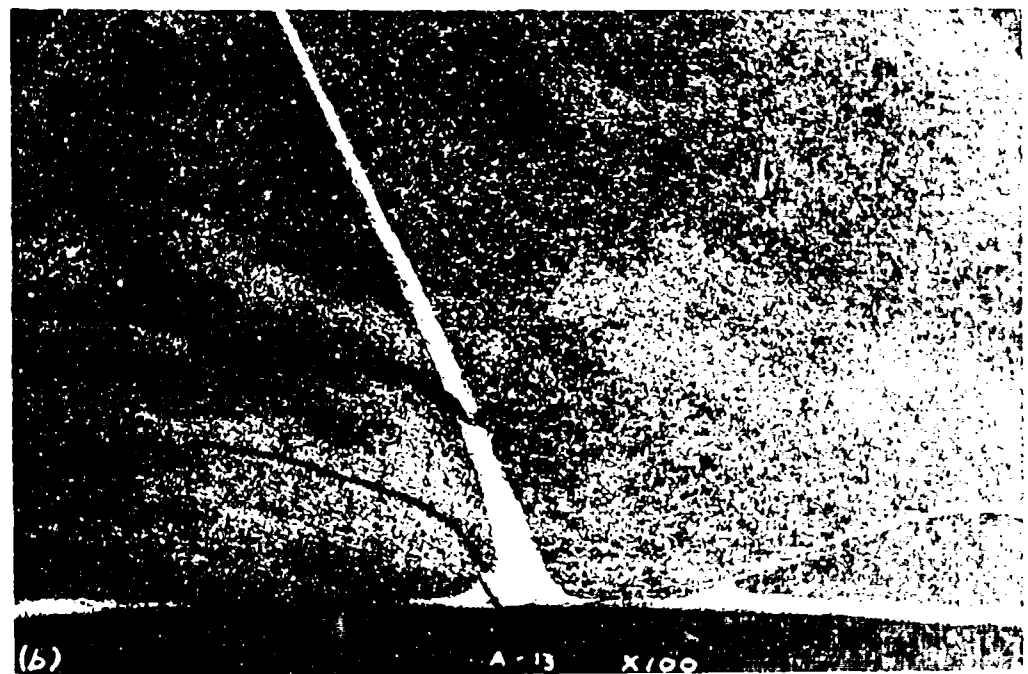
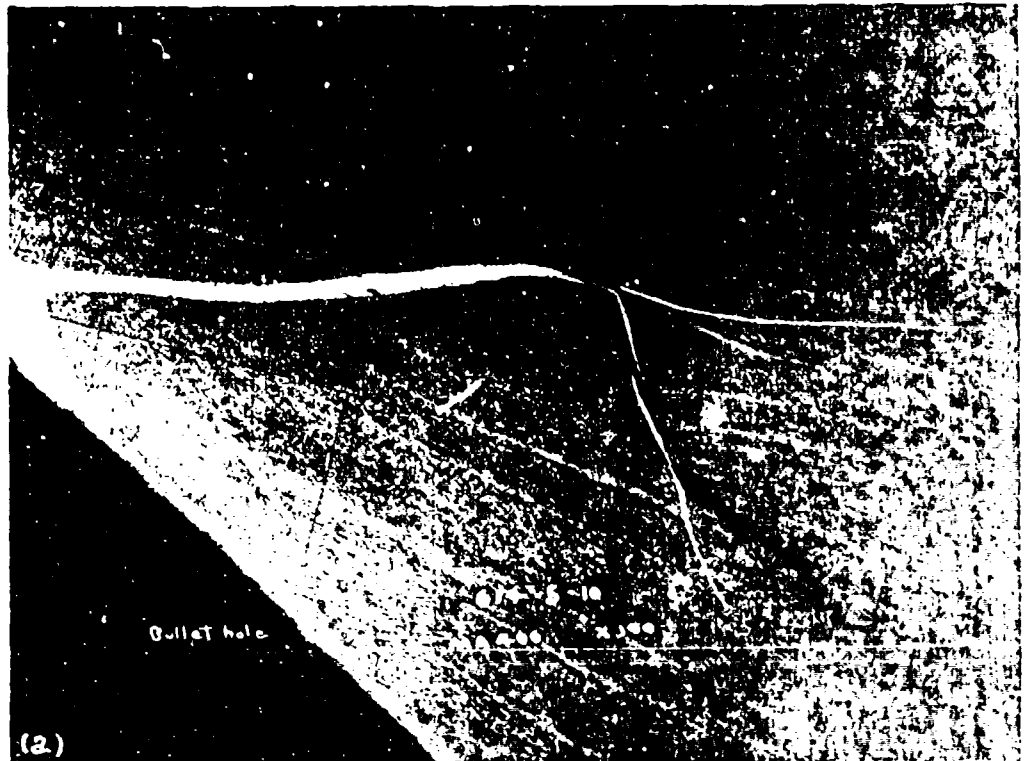
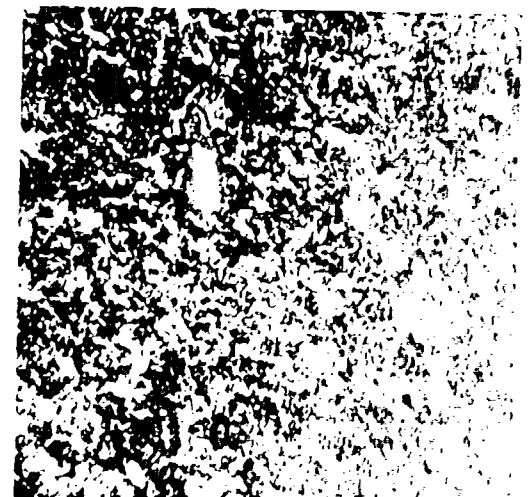
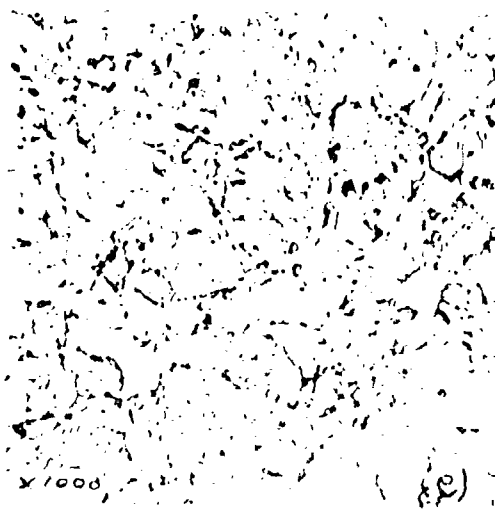
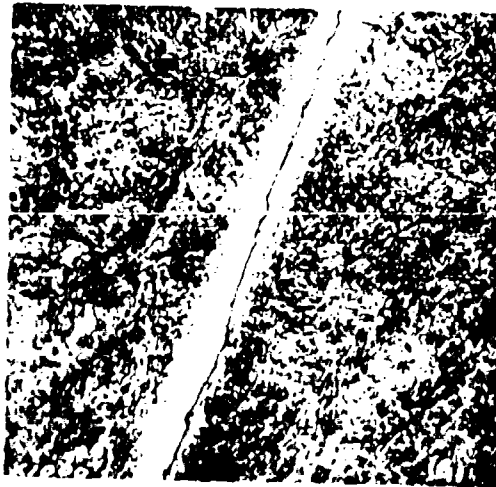
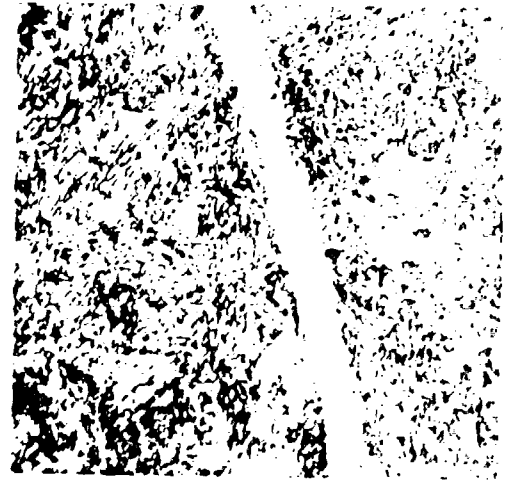
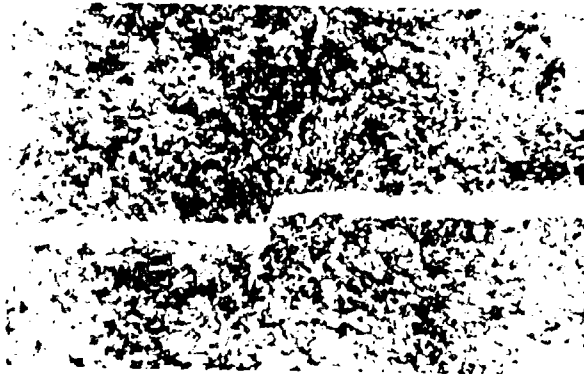


FIG 13

WA 619-1-65

Figure 14

- (a) This layer obviously was formed previous to a slipping of the metal along the plane marked by a very faint line cutting across the layer at the point of its abrupt shift.
1% Nital #614-5 Round 10 MA 406
- (b) A "white layer" at high power and, as in every case examined, no structure is discernible.
1% Nital #WJ2 Round 9 MA 167
- (c) A crack which progresses along one side of the layer, cuts across it and progresses along the other side, with no apparent cause for its termination at either end, or no indication of its origin.
1% Nital #WJ2 Round 9 MA 163
- (d) Fine crack progressing down "white layer" and swerving off to an abrupt end.
1% Nital #614-5 Round 5 MA 414
- (e) Typical microstructure of decarburized surface of armor plate away from bullet hole.
1% Nital MA 276
- (f) Typical troostite-sorbite structure of metal forced upward at bullet impact.
1% Nital MA 275



116 17

W 0 637 186

Figure 15

- (a) Elongated slag inclusions bordering "white layer". Sketch shows location of slag with respect to bullet hole. Normally, i.e. beyond the region in which the bullet exerted its influence, all the slag was elongated in the direction of rolling, that is perpendicular to the bullet penetration.

MA 714

- (b) Another nonmetallic stringer, this one penetrating into the interior of the "white layer". The deviation from a straight line upon entering into the layer suggests a "flowing" of the metal in the layer most severe at the core, but at a temperature insufficient to fuse the slag.

1% Nital #614-b Round 5c MA 713

- (c) Dark spots are actually gray-colored inclusions with smooth spherical shape in the "white layer". They have been undisturbed by the deformation of the metal. It is believed that sufficient heat has been produced in the formation of these "white layers" to melt the nonmetallics. Upon subsequent solidification, the particles assumed their normal shapes and thus presented the appearance of having been unaffected by the shock of penetration.

X3000 5% Nital #614-5 Round 8 HA1-129

- (d) Long slag stringer which stops at the "white layer". This is undoubtedly a coincidence, but it does show that the "white layer" formation does not form with any particular relation to the stringer inclusions.

1% Nital #614-5 Round 10 MA 401

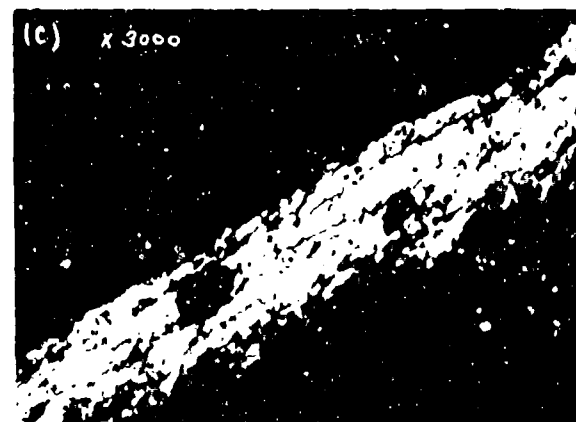


FIG 15

W A. 637-687

Figure 16

- (a) The deformation of the banding as well as the relationship of "white layers" to the cracks is especially pronounced in this micrograph. The complete absence of "white layer" in some places would indicate that the continuity of its formation was interrupted by the simultaneous growth of the crack. There is certainly in this case some relation between the cracks and layers, but just what it is, is not obvious.

1% Nitral #614-5 Round 3 MA 165

- (b) This crack in the "white layer" shows either a pulling apart of a fairly adhesive substance to form the crack, or else a torsional force acting in the crack's formation. This twisting, jagged type of crack is frequently found, and comprises about one-third of all the cracks found in layers.

1% Nitral #WJ2 Round 3 MA 168

Figure 17

Illustrating in different steels, and at various magnifications, the twisting jagged crack characteristic of a large proportion of cracks in "white layers".

- (a) This micrograph is not so clear because of the very deep etch, but it shows the twisting of crack and "white layer" at high power.

10% Nital #614-5 Round 6. MA 166

- (b) Notice the termination of the cracking at the extreme upper part of the picture. On visual examination of the rest of the "white layer" it was found to be entirely free of cracks from this point on.

Rosenhain & Haughton #29 Round 2 MA 396
MA 396

- (c) Color bandings brought out by this etch show a very definite torsional movement of the metal when examined visually. Unfortunately the photographic emulsion does not bring out the true color values, and therefore a good deal of the effect is lost.

Picric Acid etch. #WJ2 Round 3 MA 407

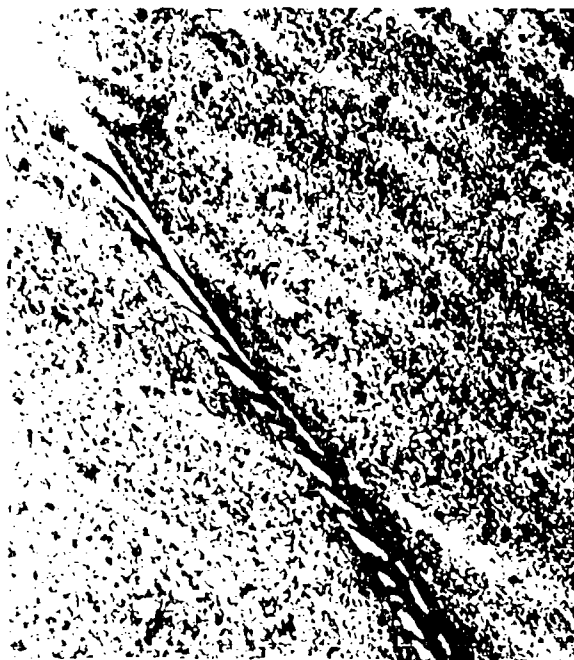


FIGURE
17



It is believed that this evidence of twist in the crack systems is the result of torsional impact. The twists in "white layers" were found near the bottom and close to the side of the bullet hole. Together with the information obtained from macro study, these pictures support the view that the spin of the bullet has exercised a torsional force on the metal.

The "white layers" are resistant to the normal procedure of etching. Relatively deep etching reveals a fine acicular structure similar to martensite in "white layers" found in an armor plate containing 3.58% nickel and 2.01% silicon, Figures 18 (d), (e) and (f). The structure of the armor plate proper was martensitic. On the other hand, the layer appearance in a standard chromium-molybdenum-vanadium armor plate is similar to that of sorbite, Figures 18 (a), (b) and (c). Their failure to exhibit an acicular structure is no proof that they lack the characteristics of hardened steels since such steels do not necessarily have to assume one definite type of structural arrangement.

The structure of this chrome-molybdenum-vanadium plate was troostite-sorbite.

High power examination after continued etching, the standard composition in 2% nital reveals the presence of fine, though rounded, detail within the "white layer" and also the presence of cracks shown in Figure 19 (c).

Figure 18

These micrographs show the best of the results from an exhaustive series of tests made to discover what, if any, method of etching would bring out the structure in these "white layers".

- (a) Very deep Nital etch. #614-5 Round 5. MA 238
- (b) Deep HCl etch. #614-5 Round 5. MA 307
- (c) Very deep HCl, HCl and HNO_3 , and finally Rosenhain and Haughton applied in that order.
#614-5 Round 10. MA 308
- (d) Deep Rosenhain and Haughton etch,
#WJ2 Round 3. MA 303
- (e) Rosenhain and Haughton, re-etched deeper than (d).
The blackened area in the lower right corner appears because the etch was so deep as to eat away the metal surrounding the "white layer".
#WJ2 Round 3. MA 304
- (f) Same as (e), but a different location in the specimen.
Note the appearance of layers within the layer.
#WJ2 Round 3. MA 305
- (g) Scratch test, showing a considerable necking down of the scratch as it passes through the "white layer".
#614-5 Round 5. MA 240

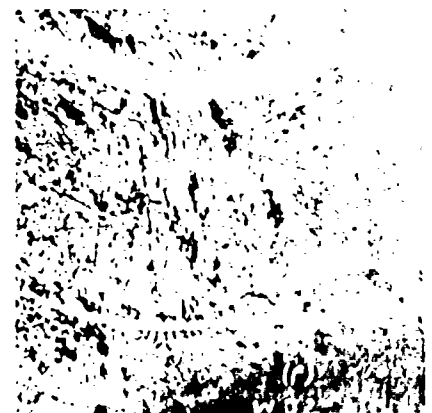
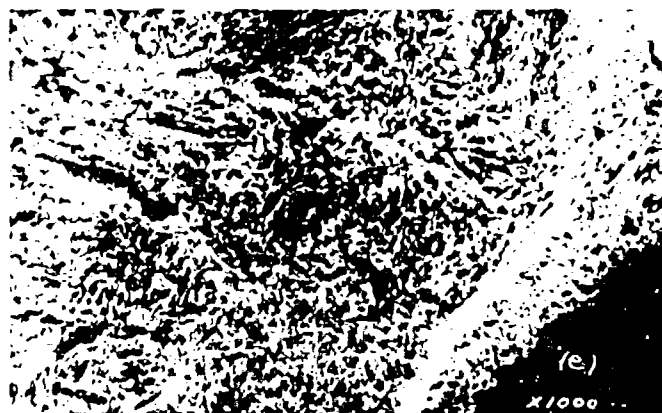
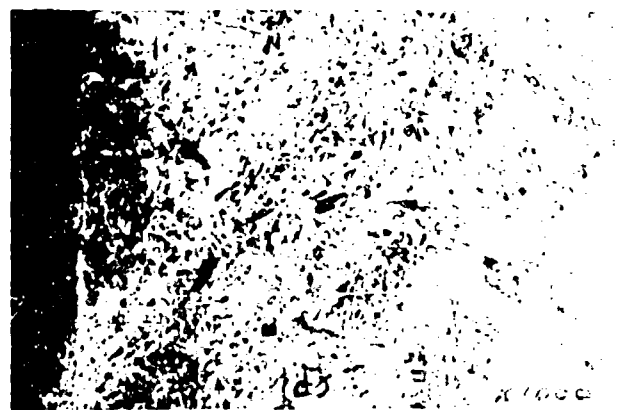
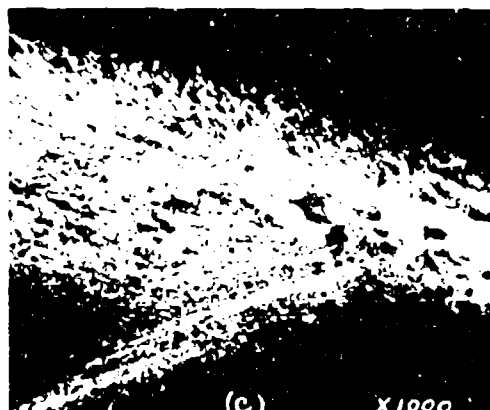
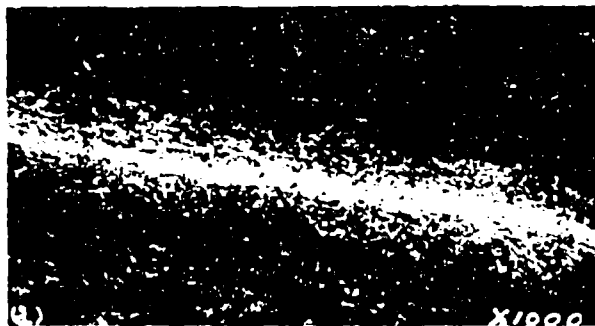


FIGURE 18

V.I.R. 621-670

A study of the "white layers" under oblique illumination revealed many interesting details which could not be detected with the use of vertical illumination. The almost complete absence of characteristic, well-defined structural outlines (see Figure 19 (a)) was noted and explained with the aid of oblique illumination by which it was possible to photograph the real surface conditions of the "white regions", Figures 19 (b) and (d). The latter were hard enough to resist the cutting action of the polishing medium. They presented to the microscope, therefore, not flat smoothly finished faces but rather irregular, cracked, furrowed ones, the structural features of which could not possibly be seen as normal metallographic outlines.

The relative hardness of the layer as compared to that of the surrounding metal is illustrated by the scratch test shown in Figure 18 (g). Moreover, the hardness of these layers is evident since they stand out in relief after metallographic polishing.

The results of this investigation indicate that these "white layers" are martensitic as the result of heat generated by slip. In this connection, it is interesting to note that E. A. Atkins found that fractured wires had been subjected to such intense friction that the skin was converted into martensite (The Journal of the Iron & Steel Institute, No. 1, 1927, Vol. CXV, p. 443).

Figure 19

- (a) Microstructure of a "white layer" in the vicinity of a bullet hole. Vertical illumination. Note absence of definite microstructure after normal etching.
2% Nital #614-5 Round 8 HAL-106
- (b) Same as in 15 (a) - Oblique illumination. Fine cracks are evident within the "white layer", also flow lines are present within and adjacent to the layer.
2% Nital #614-5 Round 8 HAL-106
- (c) Same as 15 (b) after additional etching in 2% Nital. Vertical illumination. Note presence of fine though rounded detail within the "white layer" and also the presence of cracks.
X3000 #614-5 Round 8 HAL-113
- (d) Fine detail apparent in another "white layer". Oblique illumination. Here is evidence of the furrowed condition of the surface which prevents the presentation of well-defined structural characteristics.
X3000 5% Nital #614-5 Round 8 HAL-148



W.A. 659-677

FIGURE 19.

Furthermore, N. Dawidenkow and I. Mirolubow found these "white layers" in a 0.39% carbon steel sample 13 x 13 x 7 mm which was subjected to the impact of a ram weighing 50 Kg and falling from heights between 2 and 3 meters. The authors stated, "The material of the layer finds itself in the martensitic condition only possessing no characteristic needle-like structure, because it was formed under peculiar conditions, which have not been investigated, such as high pressure and high transformation velocity." (Technical Physics of the U.S.S.R. 1935, Vol. II, p. 281). The authors also found that tempering of the layers produced structural changes and a decrease in hardness. This agrees with the results on tempering of the layers produced by bullet impact which are described below.

Tempering a standard chromium-molybdenum-vanadium armor plate at 200°C for half an hour causes a transformation at the borders of the "white layers" into a constituent which closely resembles troostite, see Figures 20 (a), (b), and (c).

Tempering this composition at 300°C for half an hour causes a nearly complete transformation of what is believed to be martensite in the "white layer" into troostite, Figures 20 (d), and (e). In several instances, the exact center of the layer was not fully transformed at the 300°C temper, see Figure 20 (e).

Figure 20

- (a) This specimen, on which the scratch tests and tempering tests were made, is shown here before either was done. The deformation of the banding is worth notice, as well as the flow lines discernible in the white coating around the tip of the bullet hole. The difference between this coating and the "white layer" is also brought out, since one of the layers can be clearly seen within this coating. Compare Fig. 7(a).

1% Nital etch #614-5 Round 5. MA 171

- (b) Same location in the specimen after tempering 30 minutes at 200°C, surface grinding, and repolishing. Here the difference between the coating and the layers has become more pronounced. The configuration of the "white layer" is of course different because of the change in the sectioning plane, but the layers originally well-defined, have begun to show a slight fuzziness at the edges, which it seems reasonable to assume, is due to the tempering action rather than the change in plane.

1% Nital etch #614-5 Round 5. MA 349

- (c) Layer structure examined closely after the 200°C temper. The fuzziness indicated in (b) shows itself as a slight etching.

1% Nital etch #614-5 Round 5. MA 325

- (d) After 300°C temper, showing a precipitation of carbides on the layer that are slightly larger than those found in the normal metal. The ease with which the layers etched after this tempering confirms the deduction from (b) and (c) that some transformation is beginning to take place.

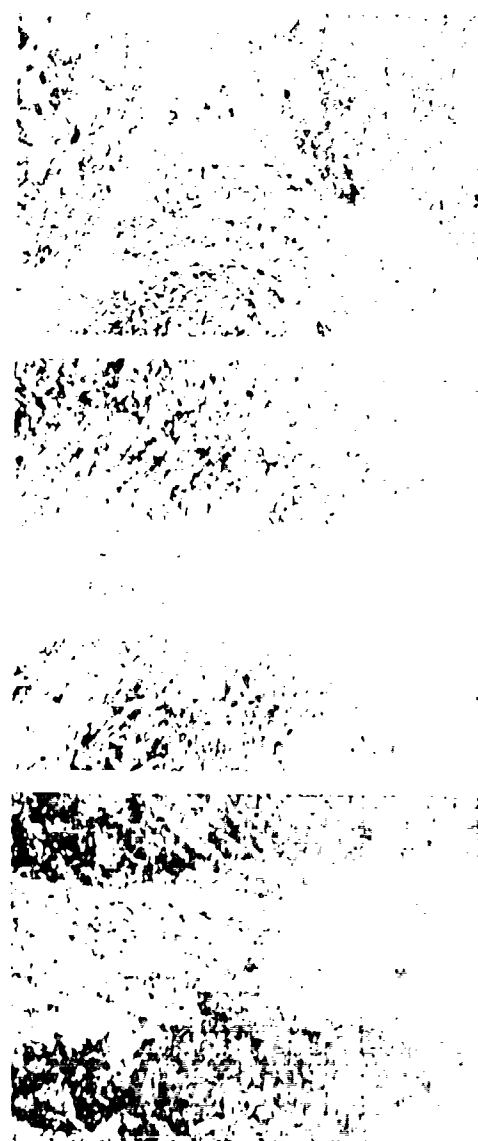
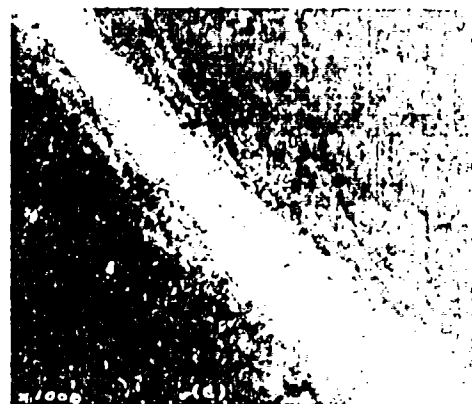
#614-5 Round 5. MA 353

- (e) Another layer in this same specimen. The fine "feather" appearance caused by flow lines on the outer portions of the layer are similar to those shown in the untempered specimen, Figure 7 (b).

1% Nital etch #614-5 Round 5. MA 354

- (f) A different composition steel, also tempered at 300°C for 30 minutes. This also shows a carbide precipitation, but more uniformly than the other specimen. Troostite-sorbite.

1% Nital etch #WJ2 Round 5. MA 365



Tempering a 3.58% nickel, 2.01% silicon composition at 300°C for half an hour promoted a complete transformation of the layer into a constituent resembling troostite-sorbite, Figure 20 (f).

After tempering, "white layers" had the following metallographic characteristics: (a) they stood out less in relief after polishing; (b) had a slightly lower resistance to abrasion; (c) did not appear to be extensively narrowed; and (d) had a greater fineness of structure.

Rolled low carbon steel plate containing 0.19% carbon, when penetrated by armor piercing bullets, is not subject to "white layer" formation.

Macroscopic examination of penetrated Hadfield's Austenitic Manganese Steel, containing 1.17% carbon and 11.40% manganese, revealed a darkened zone in the vicinity of the penetrations, Figures 21 (a), (b), (c), and (d).

Microscopic examination indicated that these darkened areas consist of carbide precipitation, deformed austenitic grains, and dark layers similar, with respect to orientation, to the "white layers" found in nonaustenitic steels, but which were darkened readily by the normal etching, see Figures 21 (e), (h), and (i).

The combined effect of severe deformation and local rise in temperature during bullet impact has evidently

Figure 21

Plate #2

- (a), (b), (c), (d), These all show a characteristic blackening about the bullet hole which is a carbide precipitation caused by heat effect of the penetrating bullet.

1% Nital etch. MA416, MA417, MA397, MA432

- (e) This is the same as Figure (d), but photographed with oblique illumination. The faulting, or slip lines revealed in this are present in all the specimens, but are partially obscured by the parallel illumination in the other photos, which was necessary to reproduce the carbide precipitation.

1% Nital etch.

MA 433

- (f) Microstructure of plate in an area far removed from the penetration.

1% Nital etch.

MA 390

- (g) A micrograph of the faulting lines reveals them to be places of dense carbide precipitation. The distortion of the structure by the impact is evident when this micro is compared to (f).

1% Nital etch.

MA 391

- (h) Carbides, precipitated out in the heat of impact, form along grain boundaries and slip lines.

1% Nital etch.

MA 394

- (i) Carbides found in selected areas as well as grain boundaries.

1% Nital etch.

MA 392

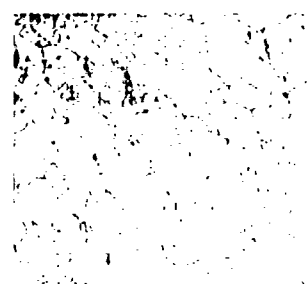
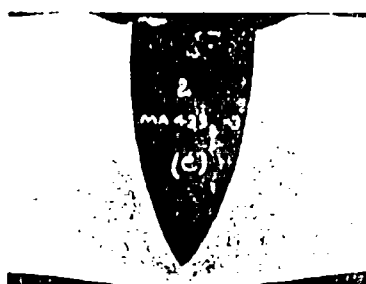
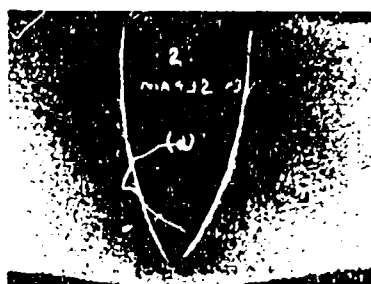
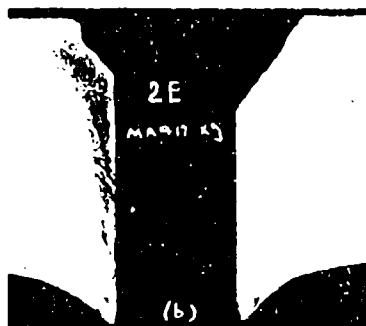
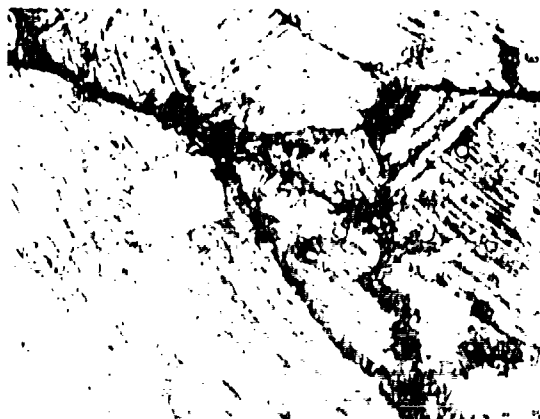
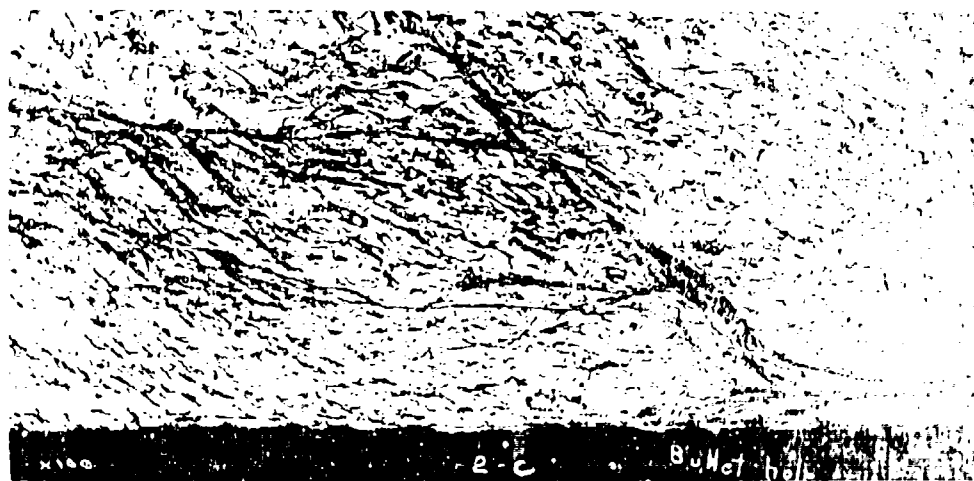


FIGURE 21.



caused decomposition of the austenite into areas containing carbide and possibly some alpha iron. Also, carbide precipitation was present at the boundaries and in the slip planes of the austenitic grains.

The structure of the manganese steel plate at considerable distance away from the bullet penetrations consists of a normal austenitic grain with no evidence of carbides at the grain boundaries, Figure 21 (f).

Microscopic examination of a cross section of bullet in plate showed no evidence of fusion of bullet core to plate. Furthermore, the effect of heat resulting from bullet penetrations on the structure of plate and core is given below:

- (1) Carbide precipitation at surface of core immediately adjacent to the plate, Figures 22 (a) and (b).
- (2) Deformed "white layer" at edge of plate in contact with bullet core, Figure 22 (a).
- (3) Decarburization occasionally found at the surface of the bullet core, Figures 22 (c) and (d).
- (4) Troostitic layer near surface of bullet core, Figures 22 (c) and (d).

It has been previously shown that bullet cores are slightly decarburized after heat treatment. Therefore, it is difficult to state definitely whether the decarburization, found in the present core stock, is due to heat of bullet impact.

Figure 22

- (a) The flow lines in the white coating on the plate's edge, as well as the indication of flow in the plate itself (upper portion of photo marked 1) is shown in contrast to the structure of jacket metal, 2, and the bullet core (lower half marked 3).

1% Nital #614-5 Round 3. MA 430

- (b) This micro shows the core and plate in complete contact at this point. Notice the carbide precipitate on the core, and flow lines in the plate.

1% Nital #614-5 Round 3. MA 159

- (c) Extreme edge of core, which shows a surface decarburization.

1% Nital #614-5 Round 3. MA 429

- (d) Structure of core 0.0005 inches from the edge. Compare with Figure (c). The blackening is due to tempering from heat generated by impact.

1% Nital #614-5 Round 3. MA 428

- (e) Crack on tip of bullet core. Compare this core structure with the structure on the sides, shown above.

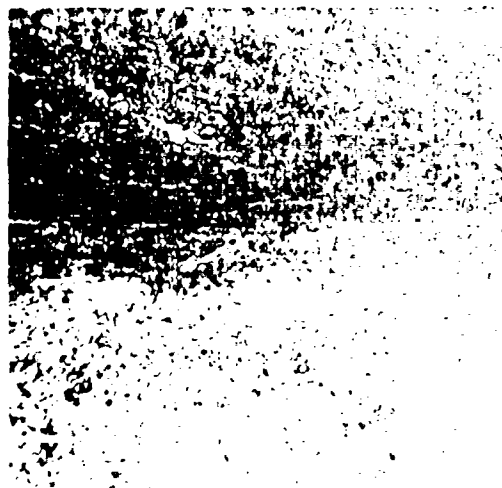
1% Nital #614-5 Round 3. MA 431

- (f) Unetched photo showing the locations of the micrographs.

1% Nital #614-5 Round 3. MA110



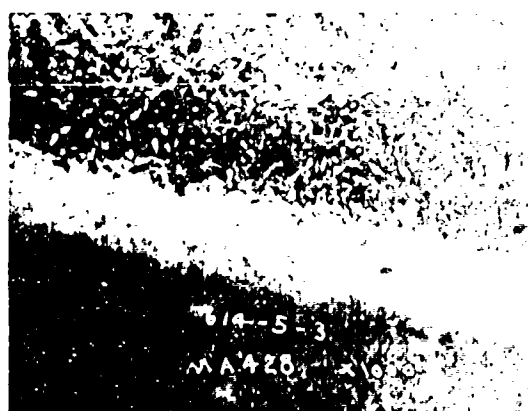
-a- X 1000



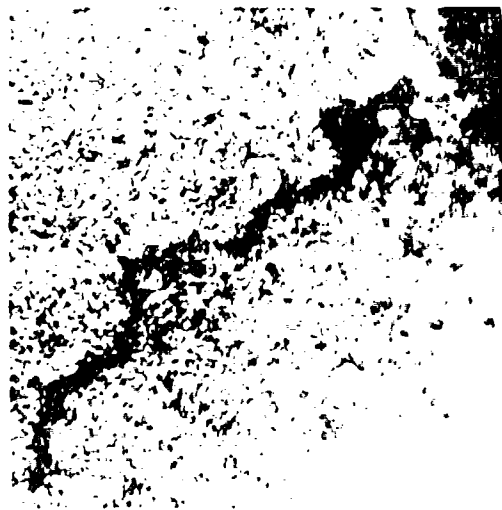
-b- X 1000



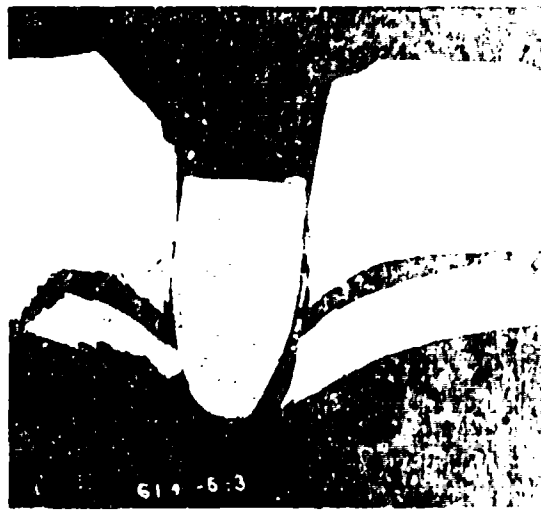
-c- X 1000



-d- X 1000



-e- X 1000



-f- X 1000

A thin layer of jacket metal located between the bullet core and plate is shown in Figure 22 (a). Figure 22 (f) shows a cross section of this bullet core in plate.

Hardness Surveys

A Vickers-Brinell hardness survey of about twenty-five penetrations of homogeneous armor plate indicates that in partially penetrated plate, the maximum hardness is in the vicinity of the tip of the penetration or near the contour of the bullet hole, representing the ogive, as noted in Figures 23, 24, 25, 26, 29, 31, and 33.

Several tests indicated that about .16 inch away from the bullet hole the hardness dropped fifteen points below the normal hardness of the plate, see Figure 27. This indicated that a tempering effect may have been produced by the heat of bullet impact. Immediately at the edge of the bullet hole, the hardness was twenty points higher than that of the plate.

Hardness surveys were occasionally made following the contour of the bullet hole, as shown in Figure 28. This particular plate spalled. The metal near the bullet hole is hardened considerably while the hardness through the

cross section of the plate from top to bottom varies as shown in Figure 28. The areas near the blowing off of the button are relatively harder.

Hardness readings near the penetration of Ex 26-1 are irregular, see Figure 30.

The hardness of areas near penetrations in Hadfield's Manganese Steel was increased in some areas about 250 points, Vickers-Brinell, Figures 31, 32. Bullet impact evidently promotes pronounced local work hardening in this steel, but not to the extent, however, to stop the bullet from penetrating the plate.

As a matter of interest, a hardness survey was made near penetrations in a low carbon steel plate, Figures 33 and 34. Curves typical of those determined on some armor plate penetrations were obtained.

A series of interesting hardness surveys were made on layers cut parallel to the surface at various depths, the same sections which were studied macroscopically, Figures 35 to 51 inclusive.

Hardness surveys at the surface of the armor plate investigated, showed that the samples were noticeably decarburized.

Hardness curves illustrate the fact previously discussed that upheaval of the metal around the bullet impact

has occurred. This metal has the hardness of heat treated armor plate while areas away from the bullet hole are relatively soft, due to decarburization. Figure 14 (f) shows the microstructure, the troostite-sorbitic structure which has been pushed upward by the bullet, while 14 (e) illustrates the structure of the normal decarburized surface.

The crater on the surface of the armor plate is metal pushed upward by the bullet. This area of disturbance on the surface coincides with the deformation revealed by macro-examination, see Figure 7 (b).

Hardness surveys on layers from the nickel-silicon plate (WJ2-4) indicated that the metal deformed around the bullet hole, as shown by a macro study, was hardened appreciably (Figures 35 - 43).

Figures 44 - 50 show that the hardness increase in the penetrated chrome-molybdenum-vanadium steel was increased to about 50 points Vickers-Brinell along the ogive. Also, the work hardened area coincides fairly well with the contour of the distorted metal as revealed by the macro-etch in Figure 7 (b).

Acknowledgement

Study of the "white layer" formation before and after tempering under very high power was made by M. R. Norton.

Respectfully submitted,

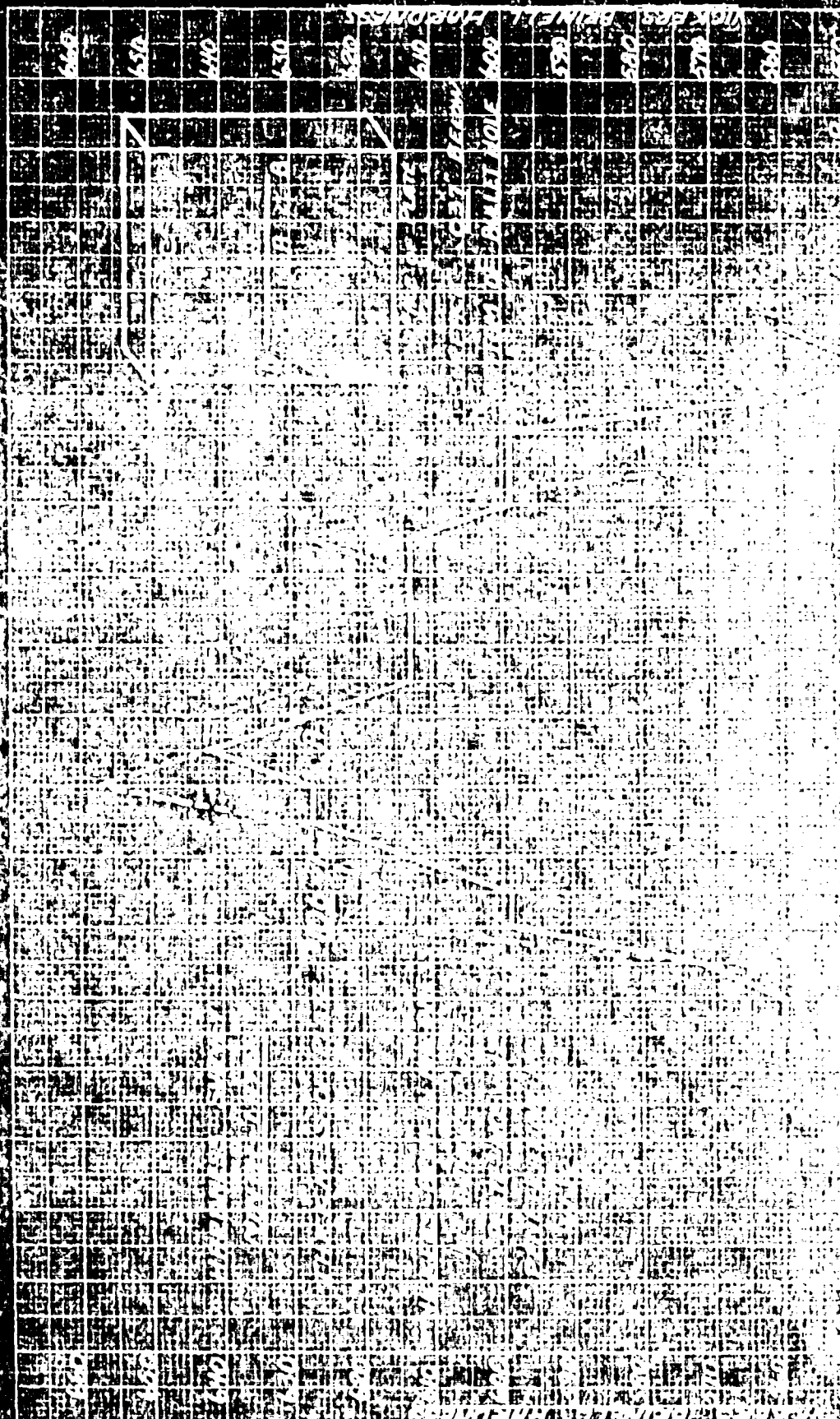
E. L. Reed

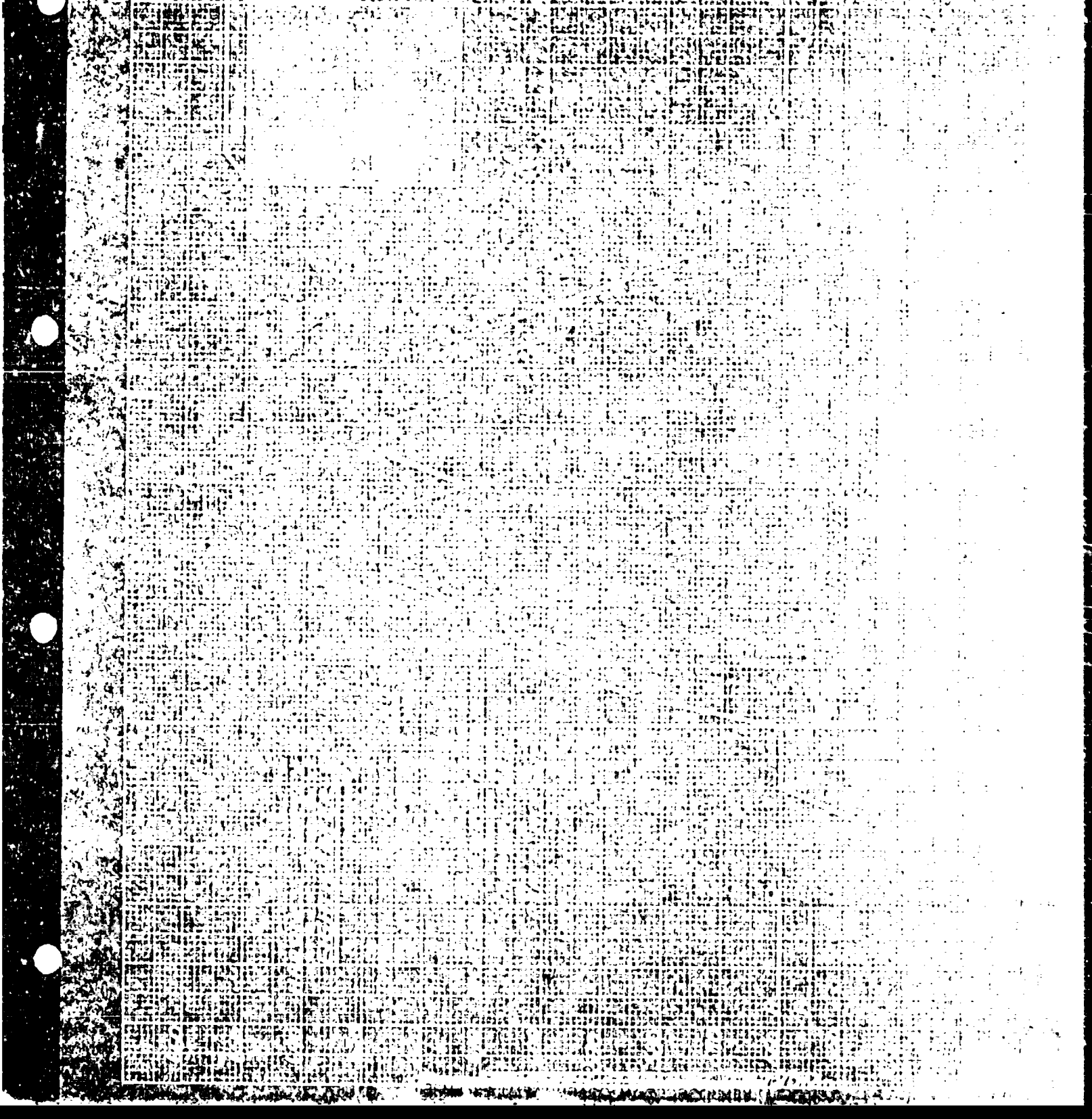
E. L. Reed,
Research Metallurgist.

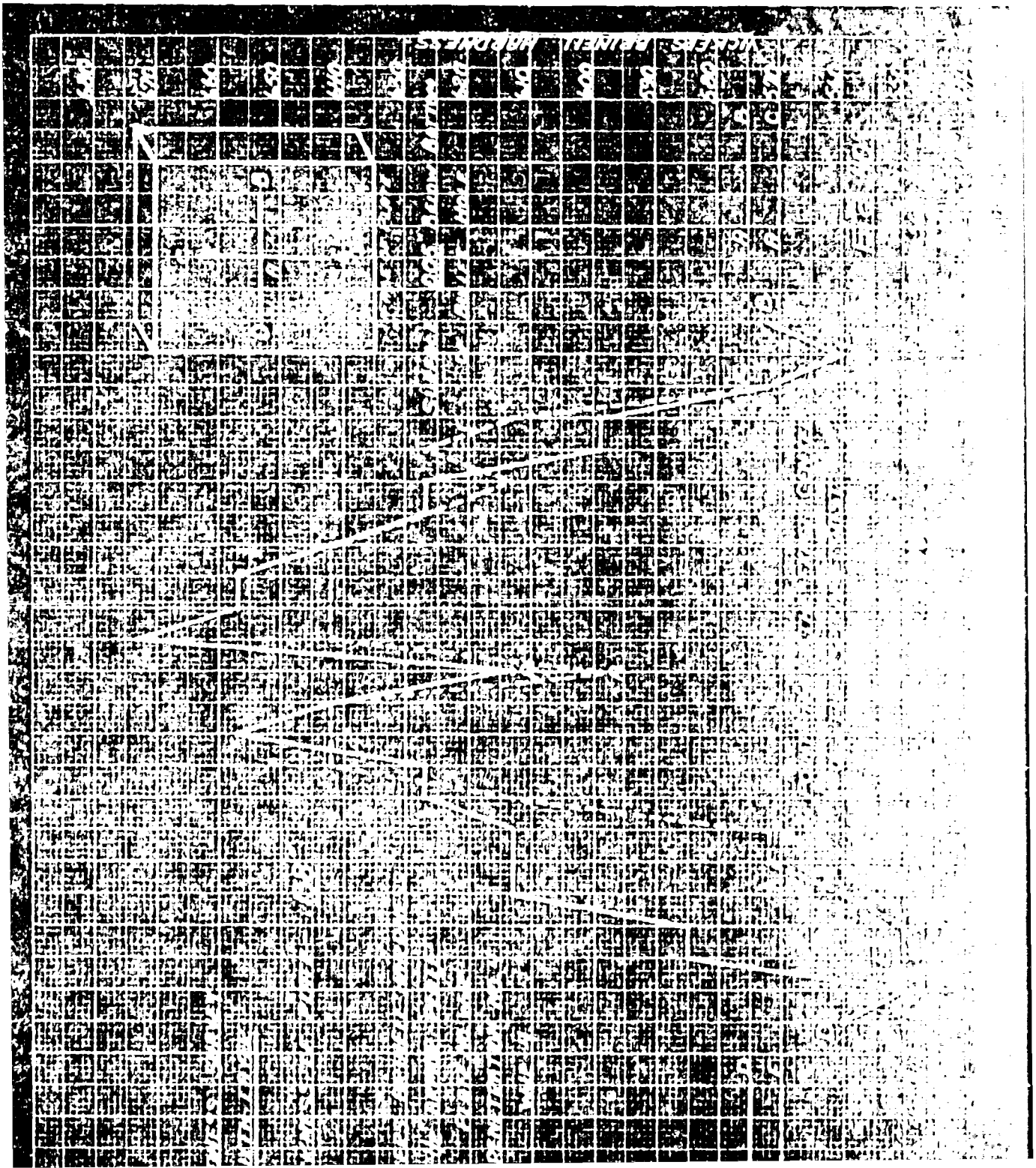
S. L. Kruegel

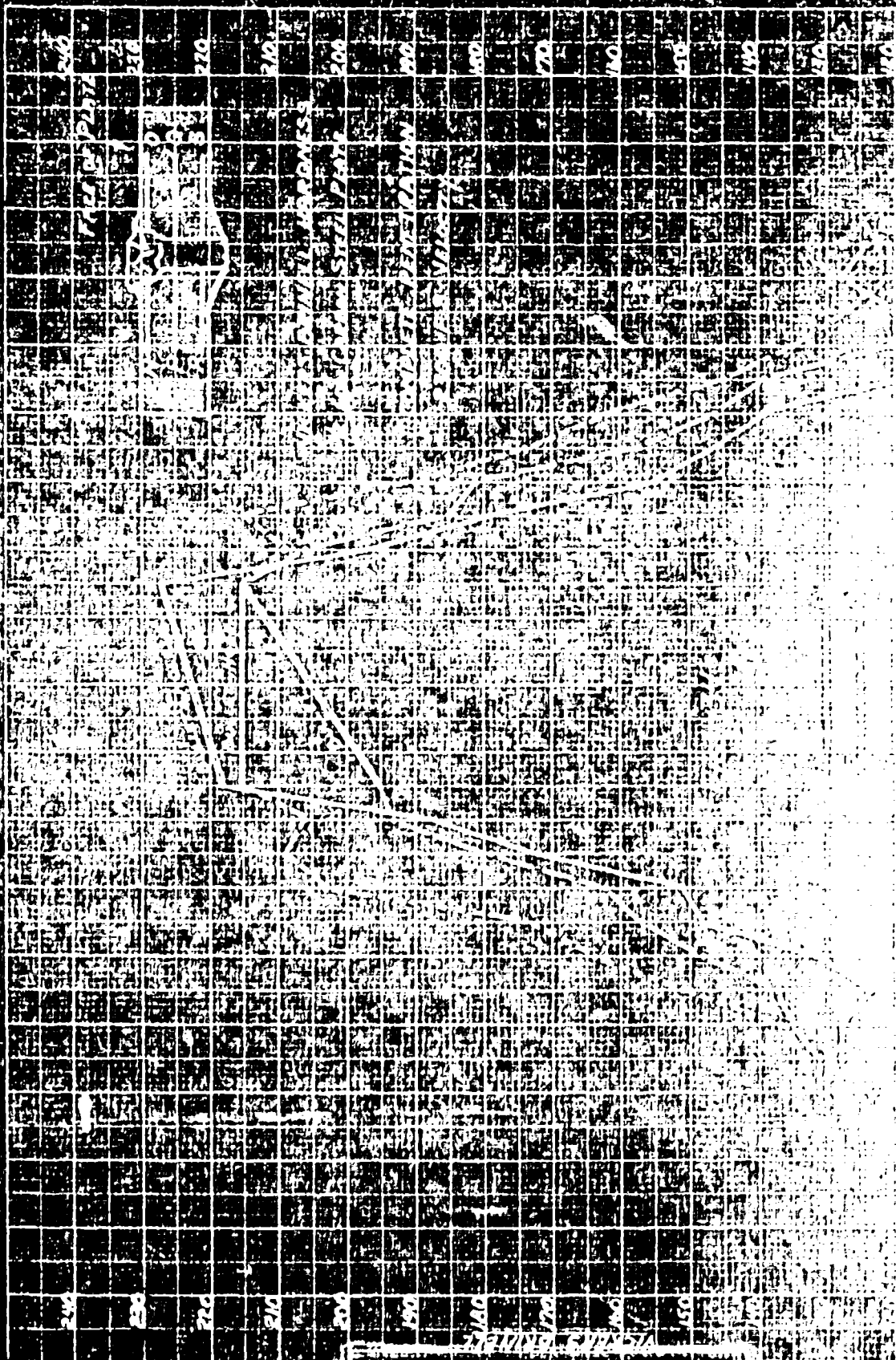
S. L. Kruegel,
Jr. Phys. Sci. Aide.

Hardness Surveys of Penetrations in
Homogeneous Armor Plate of High, Medium, and
Poor Ballistic Properties.









CARBON STEEL PLATE

Homogeneous Carbon Steel Plate.

12 x 12 x 1/2"

Brinell - 120

<u>C</u>	<u>Mn</u>	<u>Si</u>	<u>S</u>	<u>P</u>	<u>Cr</u>
.19	.42	.025	.034	.012	.05

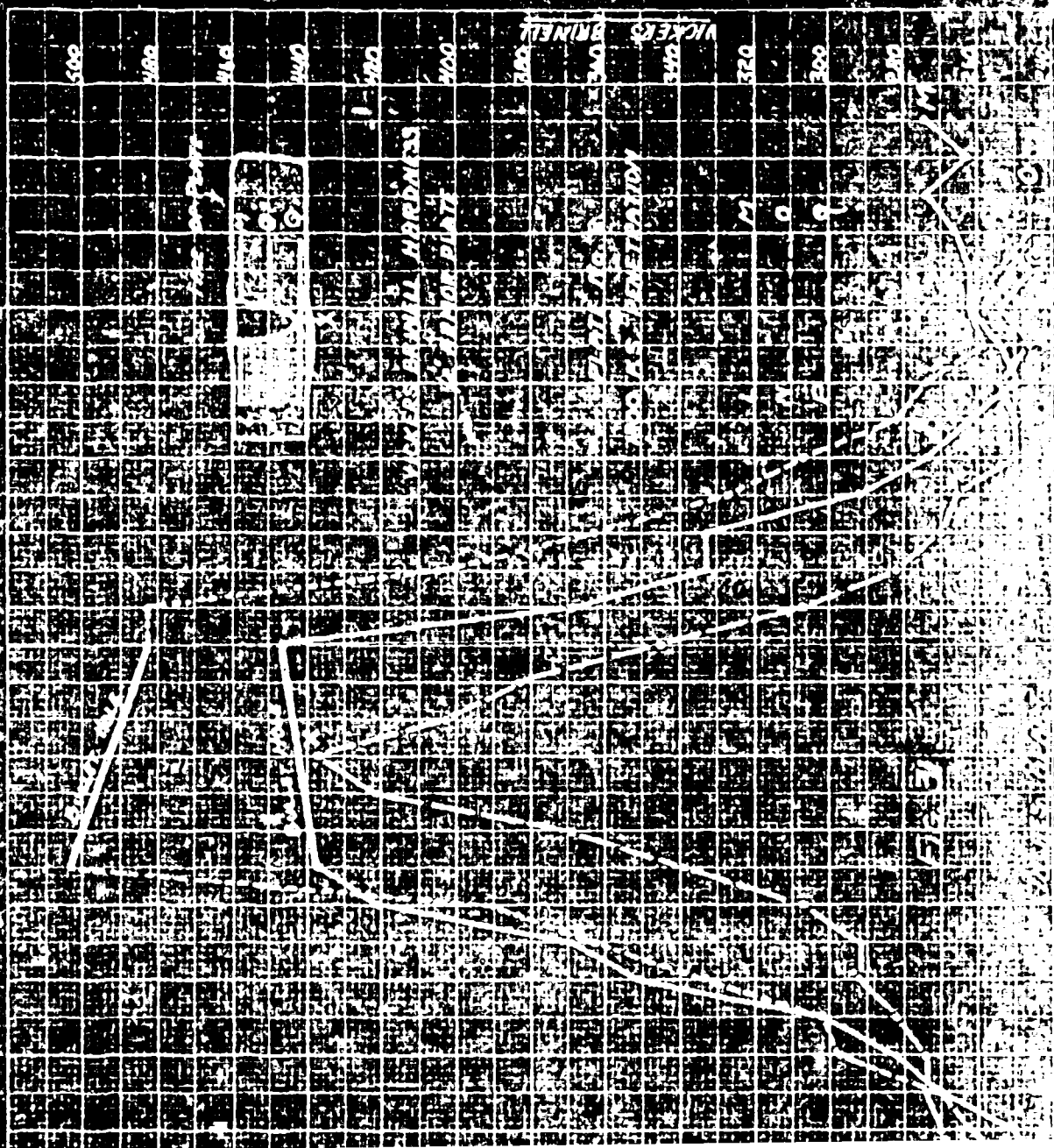
Ammunition - .30 cal. 165 gr. M1922. A.P.

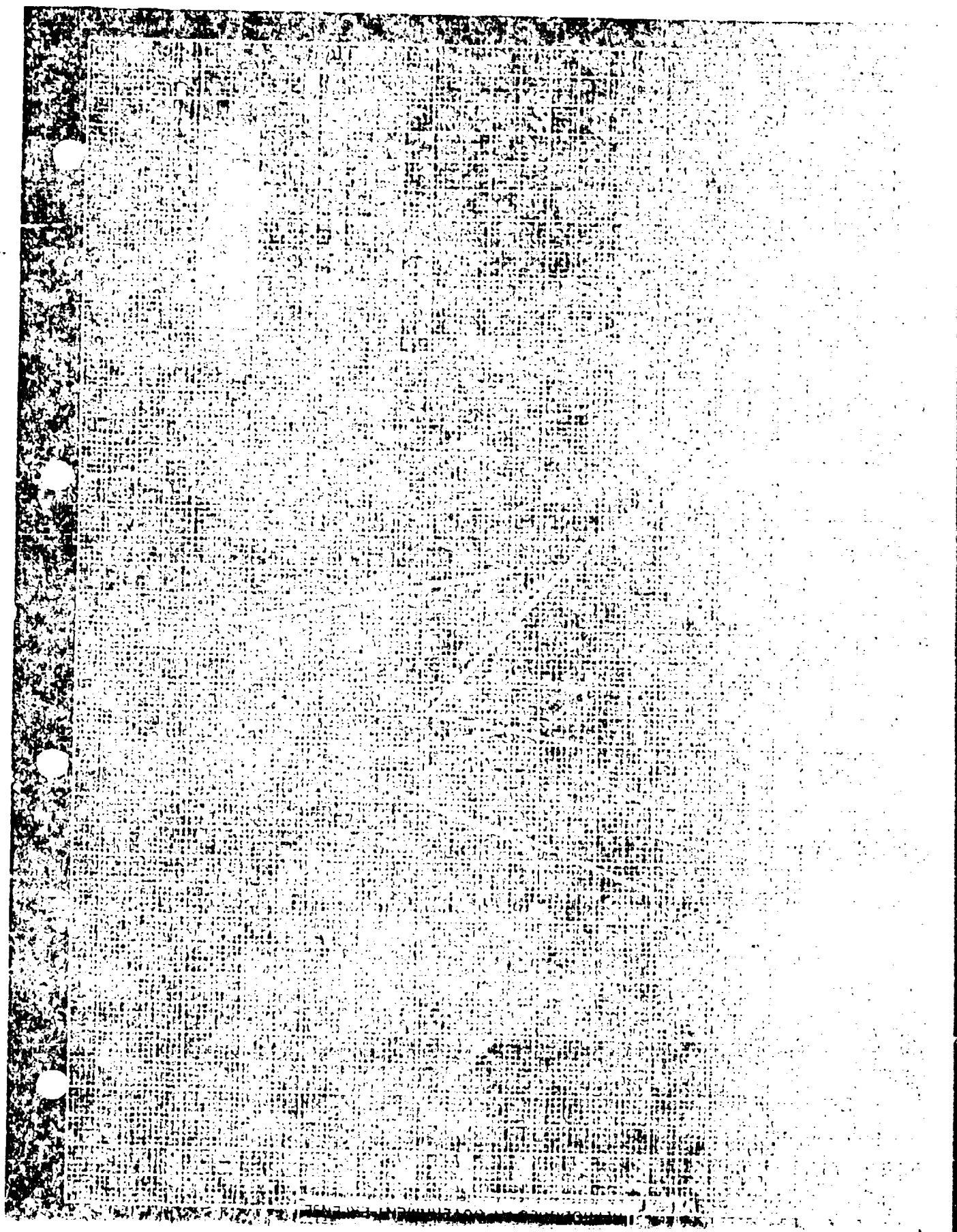
Range - 100 yards.

Specification - AXS-54, Rev. 2.

Partial Penetration - Str. Vel. 1500 f/s.

Complete Penetration - Str. Vel. 2300 f/s.





1043
FIG 26

FIG 26
343

PLATE NO. 29

High Ballistic

DISSTON - Homogeneous Armor Plate.

12 x 12 x 1"

Actual thickness - 1.0165"

Brinell - 418

<u>C</u>	<u>Mn</u>	<u>Si</u>	<u>S</u>	<u>P</u>	<u>Cr</u>	<u>Mo</u>	<u>Va</u>
.50	.70	.25	.020	.023	1.12	.65	.25

Ammunition - .50 cal. 750 gr. M-1 A.P.

Range - 100 yards.

Specification - 31.

Round 1. Str. Vel. 2499 f/s. Partial Penetration.

Height of Bulge on Back - .01"

Depth of Penetration - .77"

Round 2. Str. Vel. 2568 f/s. Partial Penetration.

Height of Bulge on Back - .05"

Depth of Penetration - .98"

Round 3. Str. Vel. 2540 f/s. Partial Penetration.

Height of Bulge on Back - .06".

Depth of Penetration - .96".

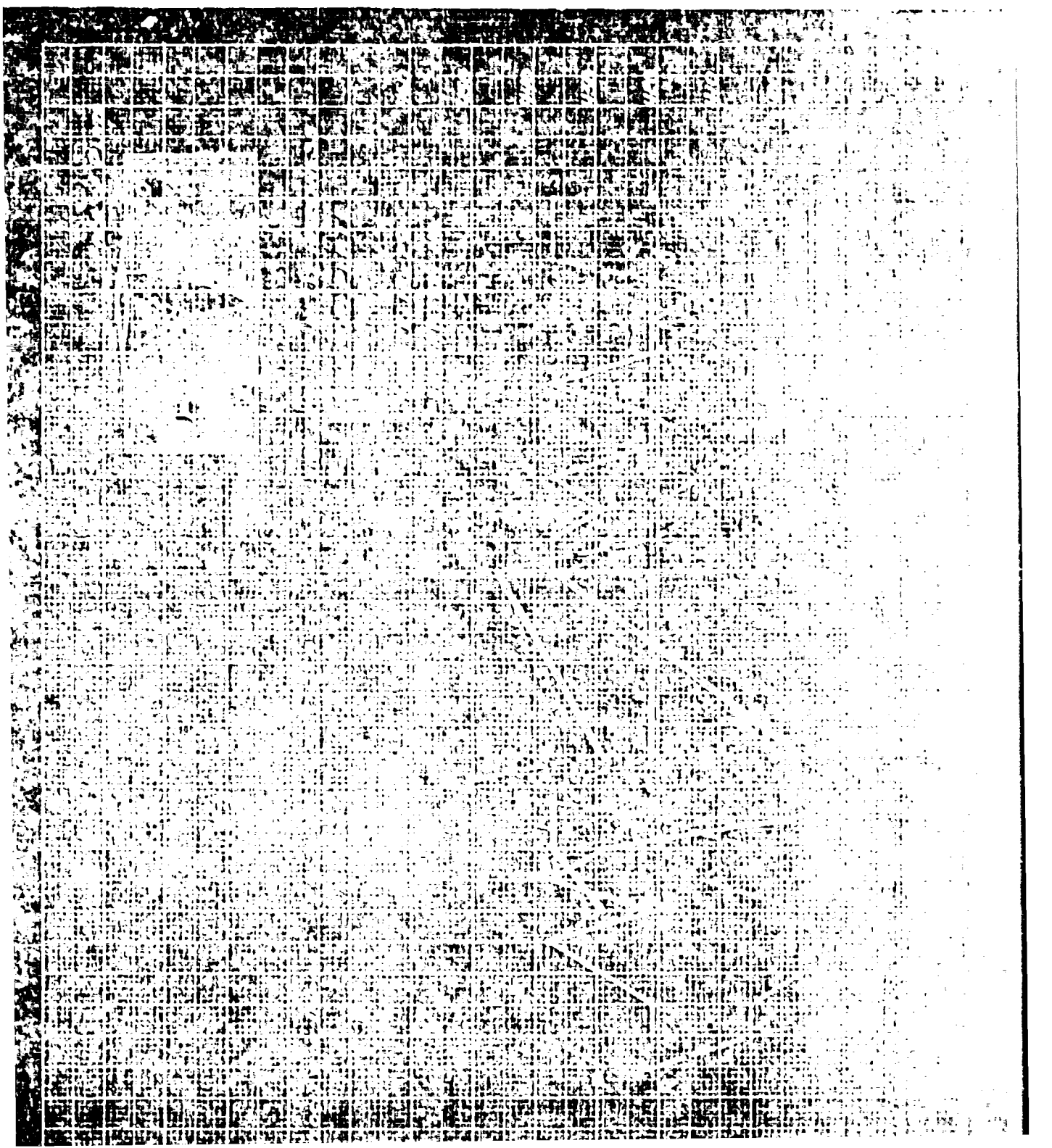


PLATE NO. WJ2

High Ballistic

JESSOP - Homogeneous Armor Plate

12 x 12 x 1/2"

Actual thickness - .496"

Brinell - 555

<u>C</u>	<u>Mn</u>	<u>Si</u>	<u>S</u>	<u>P</u>	<u>Ni</u>	<u>Cr</u>
.425	.66	2.01	.018	.024	3.58	0.24

Ammunition - .30 cal. 165 gr. M1922 A.P.

Range - 100 yards.

Specification - 31.

Round 3. Str. Vel. 2599 f/s. Partial Penetration.

Height of Bulge on Back - .01".

Round 4. Str. Vel. 2682 f/s. Partial Penetration.

Height of Bulge on Back - .01".

Round 9. Str. Vel. 2945 f/s. Partial Penetration.

Height of Bulge on Back - .01".

APPENDIX

Plate with High Ballistic Limit

Plates No. 29. WJ2

PLATE NO. 29

Size: 12 x 12 x 1 inches
Manufacturer: Henry Disston & Sons Co.
Type: Homogeneous
Ammunition: Caliber .50 A.P., 750 grain M-1
Distance from Plate to Muzzle: 100 yards
Brinell Hardness: 418
Chemical Composition:

<u>C</u>	<u>Mn</u>	<u>Si</u>	<u>S</u>	<u>P</u>	<u>Va</u>	<u>Cr</u>	<u>Mo</u>	<u>Cu</u>
C.50	0.70	0.25	0.020	0.023	0.25	1.12	0.65	0.312

Ballistics

	<u>Round 2</u>	<u>Round 3</u>
Penetration	Partial	Partial
Striking Velocity	2568 ft/sec.	2540 ft/sec.
Height of Bulge-back	0.06 inch	0.06 inch
Depth of Indent	0.98 inch	0.96 inch

Plate with High Ballistic Limit

PLATE WJ2

Size: 12 x 12 x 1/2 inches

Manufacturer: Jessop Steel Co.

Ammunition: Caliber .30 A.P., 165 gr. bullet M1922

Distance from Plate to Muzzle: 100 yards

Brinell Hardness: 555

Chemical Composition:

<u>C</u>	<u>Mn</u>	<u>Si</u>	<u>S</u>	<u>P</u>	<u>Ni</u>	<u>Cr</u>
0.425	0.66	2.01	0.018	0.024	3.58	0.24

Ballistics

	<u>Round 3</u>	<u>Round 4</u>	<u>Round 5</u>	<u>Round 9</u>
Penetration	Partial	Partial	Partial	Partial
Striking Velocity	2599 ft/sec.	2682 ft/sec.	2639 ft/sec.	2945 ft/sec.
Height of Bulge-back	-	.01 inch	0.00 inch	0.01 inch
Depth of Penetration	-	-	-	-

Plate with Medium Ballistic Limit

Plates Ex 26. 614-5

PLATE EX 26

Size: 18 x 18 x 1/2 inches
Manufacturer: Henry Disston & Sons Co.
Type: Homogeneous
Ammunition: Caliber .30 A.P. 165 grain bullet M1922
Distance from Plate to Muzzle: 100 yards
Brinell Hardness: 402 - 418

Chemical Composition:

<u>C</u>	<u>Mn</u>	<u>Si</u>	<u>Va</u>	<u>Cr</u>	<u>Mo</u>	<u>Cu</u>
0.38	0.69	0.17	0.30	1.14	0.65	0.296

Ballistics

	<u>Round 4</u>	<u>Round 5</u>	<u>Round 6</u>	<u>Round 7</u>
Penetration	Complete	Complete	Complete	Partial
Striking Velocity	2704 ft/sec.	2696 ft/sec.	2388 ft/sec.	2286 ft/sec.
Core thru back	-	0.55 inch	-	-
Core thru front	-	0.02 inch	-	-
Diameter of hole	.41 inch	-	.01 inch	-

Plate with Medium Ballistic Limit

PLATE 614-5

Size: 18 x 18 x 1/2 inches
Manufacturer: Watertown Arsenal - Henry Disston & Sons Co.
W.A. Order 8542 - Ingot 12-614
Ammunition: Caliber .30 A.P. 165 grain M1922
Distance from Plate to Muzzle: 100 yards
Brinell Hardness: 430 - 444

Chemical Composition:

<u>C</u>	<u>Mn</u>	<u>Si</u>	<u>S</u>	<u>P</u>	<u>Ni</u>	<u>Va</u>	<u>Cr</u>	<u>Mo</u>	<u>Cu</u>
0.51	0.42	0.14	0.013	0.016	0.09	0.29	1.21	0.56	0.252

Ballistics

	<u>Round 3</u>	<u>Round 5</u>	<u>Round 8</u>	<u>Round 9</u>	<u>Round 10</u>
Penetration	Complete	Complete	Partial	Partial	Partial
	C.I.P.				
Striking Velocity)	2673	2495	2391	2409	2446
	ft/sec.	ft/sec.	ft/sec.	ft/sec.	ft/sec.
Ht. Bulge-back	-	-	0.03"	0.05"	0.06"
Dia. Hole-back	-	.01"	-	-	-
Core thru back	.28"	-	-	-	-
Spalling					

Plate with Poor Ballistic Limit

PLATE NO. 2

Size: 12 x 12 x 1/2 inches
Manufacturer: Taylor-Wharton Co.
Type: Homogeneous
Ammunition: Caliber .30 A.P. 165 grain M1922
Distance from Plate to Muzzle - 50 yards
Brinell Hardness: 255

Chemical Composition:

<u>C</u>	<u>Mn</u>	<u>Si</u>	<u>S</u>	<u>P</u>
1.17	11.40	0.405	0.018	0.057

Ballistics

	<u>Round C</u>	<u>Round D</u>	<u>Round E</u>
	<u>Complete</u>	<u>Complete</u>	<u>Complete</u>
Penetration			
Striking Velocity	2215 ft/sec.	2357 ft/sec.	2283 ft/sec.
Dia. Hole-back	-	0.25 inch	-
Core thru back	.53 inch	-	0.25 inch
Core thru front	.07 inch	-	-
Ht. Bulge-back	-	0.14 inch	0.17 inch

ARMOR PLATE

(Subjected to Ball Ammunition Impact)

PLATE NO. 11 - Round 19

Size: 12 x 12 x 5/16 inches

Manufacturer: Henry Disston & Sons Inc..

Ammunition: Caliber .30 Ball M1, 110 grain bullet

Striking Velocity - 2733 ft/sec.

Diameter of Hole in back - 0.34" (complete penetration)

Distance from Plate to Muzzle: 100 yards

Brinell Hardness: 418

Chemical Composition:

<u>C</u>	<u>Mn</u>	<u>Si</u>	<u>S</u>	<u>P</u>	<u>Cr</u>	<u>Mo</u>	<u>Va</u>
0.50	0.70	0.25	0.020	0.023	1.12	0.65	0.25

LOW CARBON STEEL

(Used for Study of Deformation at Bullet Impact)

Size: 12 x 12 x 1/2 inches

Ammunition: Caliber .30 A.P. 165 grain M1922
Caliber .30 Ball Ammunition. M1

Distance from Plate to Muzzle: 100 yards.

Brinell Hardness: 120

Chemical Composition:

<u>C</u>	<u>Mn</u>	<u>Si</u>	<u>S</u>	<u>P</u>	<u>Cr</u>
0.19	0.42	0.025	0.034	0.012	0.05

PLATE NO. 614-5

Medium Ballistic

DISSTON - Homogeneous Armor Plate.

18 x 18 x 1/2"

Actual Thickness - .606"

Brinell - 430 - 444.

<u>C</u>	<u>Mn</u>	<u>Si</u>	<u>S</u>	<u>P</u>	<u>Ni</u>	<u>Cr</u>	<u>Mo</u>	<u>Va</u>
.51	.42	.14	.013	.016	.09	1.21	.56	.29

Ammunition - .30 cal. 165 gr. M1922. A.P.

Range - 100 yards.

Specification - AXS - 54.

Round 1. Str. Vel. 2696 f/s. Complete Penetration.

Diameter of Hole in Back - .70".

Round 2. Str. Vel. 2656 f/s. Complete Penetration. C.I.P.

Round 4. Str. Vel. 2459 f/s. Partial Penetration.

Diameter of Hole in Back - .005".

Round 5. Str. Vel. 2495 f/s. Partial Penetration.

Diameter of Hole in Back - .01".

Round 9. Str. Vel. 2409 f/s. Partial Penetration.

Height of Bulge on Back - .05".

Round 10. Str. Vel. 2446 f/s. Partial Penetration.

Height of Bulge on Back - .06".